Open access • Journal Article • DOI:10.2139/SSRN.1547032

Realizing Smiles: Options Pricing with Realized Volatility — Source link

Fulvio Corsi, Fulvio Corsi, Nicola Fusari, Davide La Vecchia

Institutions: University of Pisa, City University London, Northwestern University, University of St. Gallen

Published on: 17 Nov 2011 - Social Science Research Network

Topics: Volatility smile, Stochastic volatility, Implied volatility, Volatility swap and Volatility (finance)

Report

Realizing smiles: options pricing with realized volatility

LA VECCHIA, Davide, CORSI, Fulvio, FUSARI, Nicola & Swiss Finance Institute Research Series

Abstract

We develop a discrete-time stochastic volatility option pricing model, which exploits the information contained in high-frequency data. The Realized Volatility (RV) is used as a proxy of the unobservable log-returns volatility. We model its dynamics by a simple but effective (pseudo) long memory process, the Heterogeneous Auto-Regressive Gamma with Leverage (HARGL) process. Both the discrete-time specification and the use of the RV allow us to easily estimate the model using observed historical data. Assuming a standard, exponentially affine stochastic discount factor, we obtain a fully analytic change of measure. An extensive empirical analysis of S&P 500 index options illustrates that our approach significantly outperforms competing time-varying (i.e. GARCH-type) and stochastic volatility pricing models. The pricing improvement can be ascribed to: (i) the direct use of the RV, which provides a precise and fast-adapting measure of the unobserved underlying volatility; and (ii) the specification of our model, which, on the one hand, is able to accurately reproduce the volatility persistence and, on the other hand, [...]

Reference

LA VECCHIA, Davide, CORSI, Fulvio, FUSARI, Nicola & Swiss Finance Institute Research Series. *Realizing smiles: options pricing with realized volatility*. Geneva : Swiss Finance Institute Research Series, 2011, 52 p.

Swiss Finance Institute
Research Paper Series N°10 – 05

Realizing Smiles: Pricing Options with Realized Volatility

Fulvio CORSI

University of St. Gallen and Swiss Finance Institute

Nicola FUSARI

Kellogg School of Management

Davide LA VECCHIA

University of Lugano

swiss:finance:institute

FINRISK
National Centre of Competence in Research
Financial Valuation and Risk Management

Realizing Smiles: Options Pricing with Realized Volatility

Fulvio Corsi
University of St. Gallen and Swiss Finance Institute
St. Gallen, Switzerland
fulvio.corsi@usi.ch

Nicola Fusari *
Kellogg School of Management
n-fusari@kellogg.northwestern.edu

Davide La Vecchia
Universita' della Svizzera Italiana
Lugano, Switzerland
davide.la.vecchia@usi.ch

First draft: April, 2009
This draft: November 17, 2011

*Corresponding author. E-mail n-fusari@kellogg.northwestern.edu. Tel: +1 847-644-72-40. Fax: +1 847-491-5719. Department of Finance, Kellogg School of Management, Northwestern University, 2001 Sheridan Road Evanston, IL 60208. We thank an anonymous referee for helpful comments and suggestions. We are also grateful to Torben Andersen, Giovanni Barone-Adesi, Francesco Corielli, Christian Gourieroux, Peter Gruber, Patrick Gagliardini, Loriano Mancini, Nour Meddahi, Alain Monfort, Fulvio Pegoraro, Roberto Renó, Viktor Todorov, and Fabio Trojani for their constructive discussions and remarks. We also thank the participants at the SoFiE conference held in Chicago. All errors are our own responsibility. The authors acknowledge the Swiss National Science Foundation Pro*Doc program and the Swiss Finance Institute for partial financial support.

Abstract

We develop a discrete-time stochastic volatility option pricing model, which exploits the information contained in high-frequency data. The Realized Volatility (RV) is used as a proxy of the unobservable log-returns volatility. We model its dynamics by a simple but effective (pseudo) long memory process, the Heterogeneous Auto-Regressive Gamma with Leverage (HARGL) process. Both the discrete-time specification and the use of the RV allow us to easily estimate the model using observed historical data. Assuming a standard, exponentially affine stochastic discount factor, we obtain a fully analytic change of measure. An extensive empirical analysis of S&P 500 index options illustrates that our approach significantly outperforms competing time-varying (i.e. GARCH-type) and stochastic volatility pricing models. The pricing improvement can be ascribed to: (i) the direct use of the RV, which provides a precise and fast-adapting measure of the unobserved underlying volatility; and (ii) the specification of our model, which, on the one hand, is able to accurately reproduce the volatility persistence and, on the other hand, provides the necessary smoothing of the noise present in the RV dynamics.

Keywords: High-frequency, Realized Volatility, Option Pricing.

JEL Classification: C13, G12, G13

1. Introduction

It is well established that proper use of intra-day price observations leads to precise and accurate measurement and forecast of the unobservable asset volatility. At the same time, volatility is the primary ingredient of every option pricing model. In this paper, combining both these aspects, we develop a new option pricing model that effectively incorporates the information contained in high-frequency data, as summarised by the Realized Volatility (RV) measure.[1]

The RV is an easy-to-compute non-parametric measure of the asset variability, and it is typically constructed from the intra-day price movements. This allows the RV to change rapidly according to the market's movements. We show that such a reliable volatility measure yields accurate pricing of short-term options. Moreover, we show that our model is able to mimic the long-memory characterising the volatility process,[2] leading also to accurate pricing of long-term options. Thus, both the fast changing dynamics inherent in the RV and the simple long-memory structure allow our model to reproduce a realistic Implied Volatility (IV) term structure under different market conditions (e.g., different volatility regimes). The improvements on the pricing performances yielded by GARCH-type option pricing models, that rely on the volatility filtered solely from daily returns, are remarkable. Indeed, in terms of Root Mean Square Error on IV ($RMSE_{IV}$), the overall improvements on the extension of the Heston and Nandi (2000) GARCH recently proposed by Christoffersen, Jacobs, and Heston (2011) and the Component GARCH of Christoffersen, Jacobs, Ornthanalai, and Wang (2008) are 14% and 26%, respectively. Finally, the use of RV as a proxy for the unobservable volatility simplifies the estimation considerably: filtering procedures are no longer required, and the model can be estimated directly using the observed RV, as obtained from high-frequency data.

Surprisingly, to the best of our knowledge, little work has been devoted to combining RV literature with that on option pricing to construct RV option pricing models. Notable exceptions are the work of Stentoft (2008) and Christoffersen, Feunou, Jacobs, and Meddahi (2010). In Stentoft (2008), an Inverse

[1] The idea of RV measures goes back to the seminal work of Merton (1980), which shows that the integrated variance of a Brownian motion can be approximated by the sum of a large number of intra-day squared returns. This original intuition has been recently formalised and generalised by Andersen, Bollerslev, Diebold, and Labys (2001) and (2003); and Barndorff-Nielsen and Shephard (2001), (2002a), (2002b), and (2005); and Comte and Renault (1998).

[2] See, e.g., Andersen, Bollerslev, Diebold, and Labys (2001), (2003) and Andersen, Bollerslev, Diebold and Ebens (2001).

Gaussian model of a 30-minute returns RV measure is applied to price options on some individual stocks. However, this work does not provide a formal change of measure for the RV process, since it only considers the case in which the risk-neutral and physical dynamics of RV are identical (i.e., when the volatility risk is not priced). In a concurrent paper, Christoffersen, Feunou, Jacobs, and Meddahi (2010) generalise the GARCH option pricing approach by extending the Heston and Nandi (2000) GARCH model to include RV measures. However, they focus mainly on the RV's contribution to short- and medium-term option pricing.

Indeed, so far, only marginal attention has been devoted to the long-term part of the IV surface, where the persistence of the volatility process plays a crucial role. Two exceptions are Comte, Coutin, and Renault (2003), who employ a fractional stochastic volatility model, and Carr and Wu (2004), who apply alpha-stable processes to slow down the central limit theorem and obtain negative skewness and excess kurtosis for long-maturity options.

Moreover, a growing strand of literature advocates the presence of a multi-components volatility structure. For instance, Li and Zhang (2010), using non-linear principal components analysis, find that two factors are needed to explain the variation in the IV surface. Christoffersen, Jacobs, Ornthanalai, and Wang (2008) employ a modified version of the two-factor component GARCH in Engle and Lee (1999) for options pricing in discrete-time, while Bates (2000) proposes a two-factor jump-diffusion model to fit the implicit distribution in futures options. In addition, Adrian and Rosenberg (2007) show that a multi-components volatility model substantially improves the cross-sectional pricing of volatility risk.

In this paper, we combine all these streams of literature and we introduce a new class of models that rely on the RV, featuring long-memory, multi-components structure, and analytical tractability. We model the conditional mean of the volatility process by the Heterogeneous Auto-Regressive (HAR) multi-components model (see Corsi 2009). The HAR specification can be considered as an acceptable compromise between parameter parsimony and multi-components specification. Despite the fact that the HAR model does not formally belong to the class of long-memory processes, it is able to produce the same memory persistence observed in financial data. Moreover, its multi-component specification is important in providing the necessary smoothing of the otherwise too noisy (for option pricing purposes) RV measure. For these reasons the HAR has become one of the standard models for describing and

forecasting the dynamics of RV.[3] The HAR model provides only the first conditional moment of the RV. In order to specify the whole transition density and complete the probabilistic description of the RV process, we assume that the conditional distribution of the HAR is a non-central gamma. The non-central gamma is the same transition density implied by the Cox, Ingersoll, and Ross (1985) model, widely applied to describe the dynamics of the volatility process. The resulting model belongs to the family of autoregressive gamma processes, a class of discrete-time affine processes introduced by Gourieroux and Jasiak (2006). Due to this combination our new model features both long-memory and affine structure. The latter feature is particularly attractive for option pricing purposes since, as with the affine processes, leads to a fully analytic conditional Laplace transform. In order to capture the asymmetric shape of the IV smile for S&P 500 options, we include the leverage effect. The resulting model is extremely flexible for option pricing purposes. Moreover, considering restricted versions of this general model, we are able to disentangle the contribution of the different model ingredients (i.e. long memory and leverage) to the overall pricing performance.

The paper is organised as follows. Section 2 defines our model for log-return and RV under both the historical and risk-neutral probability measures. Section 3 describes the estimation of the model, and then analyses its dynamic features. In Section 4, we present the option pricing performances, compare them with option pricing benchmarks, and perform several robustness checks. Finally, Section 5 summarises the results.

[3] Andersen, Bollerslev, and Diebold (2007), Aït-Sahalia and Mancini (2008), McAleer and Medeiros (2008), Busch, Christensen, and Nielsen (2010), and Andersen, Bollerslev, and Huang (2010) use this model (and its extensions) to forecast the RV; Clements, Galvão, and Kim (2008) and Maheu and McCurdy (2010) implement it for risk management; Bollerslev, Tauchen, and Zhou (2009) use it to analyse the risk-return trade-off; Andersen and Benzoni (2010) employ it to test whether bond yields span volatility risk; and Bollerslev and Todorov (2011) adopt it for modelling the expected Integrated Volatility to compute the Investor Fear Index.

2. The model

2.1. Dynamics under physical probability

2.1.1. Log-return dynamics

A well-established result in financial econometrics literature is that the marginal distribution of daily log-return is not Gaussian but typically features fat tails (leptokurtic distribution). This fact has motivated the use of heavy-tailed distributions in several financial models. In spite of this consideration, Clark (1973) and Ane and Geman (2000) theoretically argue that, for an underlying continuous-time diffusion process, the standard Gaussian distribution can be recovered by rescaling the log-return by an appropriate measure of the market activity. The basic intuition is that the log-return process is a Brownian motion with a random time. Rescaling the log-return by an appropriate activity measure is equivalent to performing a time-change that restores the standard Brownian motion in calendar time. As such a measure of market activity, we adopt the continuous component of the total variation of the log-price process, i.e., the Integrated Variance ($\mathcal{IV}$). Then, we assume the following conditional dynamics for the log-return:

$$y_{t+1} := \ln\left(\frac{S_{t+1}}{S_t}\right) = \mu_{t+1} + \sqrt{\mathcal{IV}_{t+1}}\epsilon_{t+1}, \tag{1}$$

$$\epsilon_{t+1}|\,\mathcal{IV}_{t+1} \sim N(0,1).$$

In our notation, y_{t+1}, S_{t+1}, and $\mathcal{IV}_{t+1}$ are the cum-dividend log-return, the price, and the $\mathcal{IV}$ at time $t+1$, respectively. For the drift of the log-return under the physical measure, we propose the following specification:

$$\mu_{t+1} = r + \left(\tilde{\gamma} - \frac{1}{2}\right)\mathcal{IV}_{t+1}, \tag{2}$$

where r represents the risk-free rate between t and $t+1$, and $\gamma := \tilde{\gamma} - 1/2$. The term $-1/2$ in γ is a convexity adjustment introduced such that the conditional expectation of returns becomes $\mathbb{E}\left[\exp y_{t+1}|\mathcal{IV}_{t+1}\right] = \exp\left(r + \tilde{\gamma}\mathcal{IV}_{t+1}\right)$ and $\tilde{\gamma}$ can be interpreted as the price risk for volatility. We observe that our specification introduces a contemporaneous effect of $\mathcal{IV}_{t+1}$ on y_{t+1}. Specifically, the functional form we are proposing implies a stochastic drift, changing with the daily $\mathcal{IV}$. This feature has an interesting probabilistic implication, since our model can be embedded into the class of nor-

mal variance-mean mixture, with $y_{t+1}|\mathcal{IV}_{t+1} \sim N\left(r + \left(\tilde{\gamma} - \frac{1}{2}\right)\mathcal{IV}_{t+1}, \mathcal{IV}_{t+1}\right)$; see, e.g., in Barndorff-Nielsen, Kent, and Sorensen (1982).

As it is customary in RV literature, we estimate the unobservable $\mathcal{IV}$ by the corresponding continuous component of daily RV (details on the RV measure employed in the implementation of the model are given in Section 3.2.). This choice has also an empirical justification. Andersen, Bollerslev, Diebold, and Labys (2000), (2001), and (2003), Andersen, Bollerslev, Diebold, and Ebens (2001), and Andersen, Bollerslev, and Dobrev (2007) indeed showed that, when daily returns are standardised by the corresponding daily RV, the resulting distribution is nearly Gaussian. We observe the same feature for our S&P 500 data, as can be seen clearly from the density plots of Fig. 1. Besides the graphical evidence, we also note that the values of the kurtosis are 7.32 and 3.68 for actual and for rescaled log-return, respectively. However, the Shapiro-Wilks test does not accept the assumption of normality. This rejection is in line with the result of Andersen, Bollerslev, and Dobrev (2007) who show that to completely restore the normality one should take into account for jumps in returns and leverage effects.

[Figure 1 should be here]

2.1.2. Realized volatility dynamics

Under the physical measure, the model is completed by specifying the dynamics of the RV process. To capture the well-documented feature of strong persistence in volatility, we follow Corsi (2009), and we model the conditional mean of the RV (given its past values) using the conditional expected value of a HAR process. The HAR model for RV is a multi-components volatility model specified as a sum of different volatility components defined over different time horizons. Specifically, the structure of the HAR model allows us to separate short-, medium-, and long-term volatility components. This feature has considerable option pricing implications as documented by Bollerslev and Mikkelsen (1996) and Comte, Coutin, and Renault (2003). In addition, Adrian and Rosenberg (2007) show that a multi-components volatility model substantially improves the cross-sectional pricing of volatility risk. Finally, to take into account the asymmetry in the smile, we here extend the original HAR model by including a daily leverage effect.

For option pricing purposes, we need the specification of the whole transition probability density or,

equivalently, the specification of the conditional characteristic function. Therefore, we model RV as an autoregressive gamma process (see Gourieroux and Jasiak 2006), with p-lags. In our model we set $p = 22$. Consequently, RV_{t+1} features a non-central Gamma transition distribution $\Gamma(\delta, \beta'(\mathbf{RV}_t, L_t), c)$, with shape and scale parameters δ and c, respectively, and location given by:

$$\beta'(\mathbf{RV}_t, L_t) = \beta_1 RV_t + \beta_2 RV_t^w + \beta_3 RV_t^m + \beta_4 L_t \tag{3}$$

where $\beta := (\beta_1, \beta_2, \beta_3, \beta_4)' \in \mathbb{R}^4$, $RV_t^w := \sum_{i=1}^{4} RV_{t-i}/4$, $RV_t^m := \sum_{i=5}^{21} RV_{t-i}/17$, and $\mathbf{RV}_t := (RV_t, RV_t^w, RV_t^m)$ is a column vector in $\mathbb{R}^3$. The quantity L_t represents the leverage effect $L_t := I_{(y_t<0)} RV_t$ (where $I_{(y_t<0)}$ takes value 1 if the log-return at date t is negative and takes value 0 otherwise).[4]

The conditional mean and conditional variance are given by:

$$\mathbb{E}_t(RV_{t+1}) = c\delta + c(\beta_1 RV_t + \beta_2 RV_t^w + \beta_3 RV_t^m + \beta_4 L_t), \tag{4}$$

$$\mathbb{V}_t(RV_{t+1}) = c^2\delta + 2c^2(\beta_1 RV_t + \beta_2 RV_t^w + \beta_3 RV_t^m + \beta_4 L_t). \tag{5}$$

In the same spirit as Corsi (2009), the specification in Eq. (3) collects the lagged terms in three different non-overlapping factors: RV_t (short-term volatility factor), RV_t^w (medium-term volatility factor), and RV_t^m (long-term volatility factor). Although different from the standard HAR parametrisation, the parametrisation in Eq. (3) does not imply any loss of information compared to the original in Corsi (2009), since it relies only on a different rearrangement of the terms. We thus label this model as the Heterogeneous Autroregressive Gamma with Leverage (HARGL).

Thanks to the strong analytical tractability of the HARGL specification, we can write down in closed-form the one-step-ahead conditional Laplace Transform (LT) under $\mathbb{P}$. In particular, from computations similar to those in Gagliardini, Gouriéroux, and Renault (2011), the conditional LT of an HARGL process is:

$$\varphi_{RV}^{\mathbb{P}}(\eta) := \mathbb{E}(\exp(-\eta RV_{t+1})|(\mathbf{RV}_t, L_t)) = \exp\left(-\frac{c\eta}{1+c\eta}\left(\beta'(\mathbf{RV}_t, L_t) - \delta\ln(1+c\eta)\right)\right), \tag{6}$$

[4]This leverage specification has been introduced by Engle and Gallo (2006). Despite assuring the positivity of the process, this specification differs from the one used in GARCH models. The HARGL leverage specification is less persistent than the GRACH one, since the former depends only on the past log-return, while the latter depends on the level of the volatility.

where $\eta \in \mathbb{R}$ and $\beta'(\mathbf{RV}_t, L_t)$ as in (3).

Restricted versions of the HARGL are easy to obtain: setting $\beta_4 = 0$ gives the HARG model which preserves the long-memory property but loses the leverage effect; with $\beta_2 = \beta_3 = \beta_4 = 0$ we obtain the simple autoregressive gamma model of order one (ARG) which is the exact discrete-time version of the CIR process; setting $\beta_2 = \beta_3 = 0$ leads to an autoregressive gamma of order one with leverage (ARGL). Both HARG and ARG models belong to the class of affine processes, thus, from Eq. (6), it is possible to derive in closed-form the multi-step-ahead conditional LT.[5]

We remark that the need for the conditional LT of RV under the physical measure is twofold. First, from the probabilistic point of view, the conditional LT completely characterises the distributional features of the RV (e.g. it uniquely defines its conditional moments and its transition density). Second, the conditional LT of RV is important for option pricing purposes, as it is a necessary tool to describe the joint behavior of the log-return process and RV needed in the change of probability measure.

2.1.3. Joint conditional Laplace transform

Given the setup outlined in Sections 2.1.1. and 2.1.2., our model specification is:

$$\begin{aligned} y_{t+1}|RV_{t+1} &\sim N\left(r + \left(\tilde{\gamma} - \frac{1}{2}\right) RV_{t+1},\ \ RV_{t+1}\right), \\ RV_{t+1}|\mathcal{F}_t &\sim \Gamma(\delta, \beta'(\mathbf{RV}_t, L_t), c), \\ \beta'(\mathbf{RV}_t, L_t) &= \beta_1 RV_t + \beta_2 RV_t^w + \beta_3 RV_t^m + \beta_4 L_t. \end{aligned} \tag{7}$$

In this section, to complete the probabilistic description of the log-return and RV dynamics, we study the joint process $K'_{t+1} := (y_{t+1}, RV_{t+1})$. This is a bi-dimensional, real-valued process of log-return and RV whose state space is $\mathbb{R} \times \mathbb{R}^+$. For the sake of notation, let $\mathcal{F}_t := \sigma(y_t, RV_t)$ indicate the σ-algebra containing the information about (y_t, RV_t) available at time t. Thanks to our model setup, we can easily obtain a closed-form expression for the conditional LT of K'_{t+1}. Proposition 1 defines the closed-form expression for the conditional LT of K'_{t+1}.

[5] Due to the presence of the leverage effect, an analogous closed-form formula is not available for the multi-step-ahead conditional LT of the HARGL. The HARGL is, however, easy to simulate, following the method illustrated in Gourieroux and Jasiak (2006).

Proposition 1. *If* $RV_{t+1}|\mathcal{F}_t \sim \Gamma(\delta, \beta'(\mathbf{RV}_t, L_t), c)$*, then the conditional LT of* $K'_{t+1} := (y_{t+1}, RV_{t+1})$ *in* $\alpha' = (\alpha_1, \alpha_2) \in \mathbb{R} \times \mathbb{R}$ *under the physical measure* $(\mathbb{P})$ *is, for* $v \in \mathbb{R}$*:*

$$\varphi_K^{\mathbb{P}}(v) = exp(-b(v) - a(v)\beta'(\mathbf{RV}_t, L_t)), \tag{8}$$

with $v = \alpha_2 + \gamma\alpha_1 - \alpha_1^2/2$ *and the terms* $b(v)$ *and* $a(v)$ *given by*

$$b(v) = \delta \ln(1 + cv) \tag{9}$$

and

$$a(v) = \frac{cv}{1 + cv}. \tag{10}$$

Proof. See Appendix A1. □

This is an important result, since the joint conditional LT provides us with a complete characterization of the joint conditional (namely, given $\mathcal{F}_t$) transition probability that can be applied to derive an explicit one-to-one mapping between the parameters of (y_{t+1}, RV_{t+1}) under the measures $\mathbb{P}$ and $\mathbb{Q}$ as described in the next section.

2.2. Risk-neutral dynamics

The risk-neutral dynamics of both the log-return and the RV process are obtained following the direct approach of Bertholon, Monfort, and Pegoraro (2008). We adopt a straightforward modification of a standard, discrete-time exponential affine SDF for the time $(t, t+1)$ applied, e.g., in Gagliardini, Gouriéroux, and Renault (2011) and Gourieroux and Monfort (2007). Due to the model dynamics described in Eq. (7), we introduce a SDF involving both the log-return and RV at $t+1$. More precisely, assuming $r = 0$ for computational convenience, we specify the following SDF:

$$M_{t,t+1} = \frac{\exp(-\nu_1 RV_{t+1} - \nu_2 y_{t+1})}{\mathbb{E}_t^{\mathbb{P}}\left[\exp(-\nu_1 RV_{t+1} - \nu_2 y_{t+1})\right]}, \tag{11}$$

where $\mathbb{E}_t^{\mathbb{P}}[\cdot]$ represents the conditional expectation $\mathbb{E}[\cdot|\mathcal{F}_t]$ under the physical measure $\mathbb{P}$.
Under specific restrictions on the vector $\nu \in \mathbb{R}^2$, we state:

Proposition 2. *Under the model specification in Eq. (7), the SDF in (11) is compatible with the no-arbitrage conditions, provided that suitable parameter-restrictions are satisfied. The parameter* ν_1 *remains a free parameter.*

Proof. See Appendix A2. □

The last proposition shows that the SDF in (11) complies with the no-arbitrage conditions. Given the market incompleteness and the results in Proposition 2, the only free parameter is ν_1.

Moreover, thanks to the SDF specification in Eq. (11), it is possible to write down in closed-form the dynamics of RV under the martingale measure. To this end, we rely on the results in Proposition 1 and specify the conditional LT under $\mathbb{Q}$ of the joint process K_{t+1}. We then have:

Proposition 3. *Under the R.N. probability measure $\mathbb{Q}$, the RV is still a HARGL, having parameters*

$$\begin{aligned} \beta^* &= \frac{\beta}{(1+c\lambda)^2}, \\ \delta^* &= \delta, \\ c^* &= \frac{c}{1+c\lambda}, \end{aligned} \tag{12}$$

with $\lambda = \nu_1 + \frac{\gamma^2}{2} - \frac{1}{8}$ and $\beta \in \mathbb{R}^4$ as in Eq. (3).

Proof. See Appendix A3. □

The last proposition provides in Eq. (12)-(12) the explicit formulas for the one-to-one mapping between the parameters of the RV under $\mathbb{P}$ and $\mathbb{Q}$. The availability of such formulas is a consequence of the affine specification of the SDF and of the high analytical tractability of the HARGL process. From the previous results, we can finally conclude:

Corollary 4. *Under $\mathbb{Q}$, the log-return follows a discrete-time stochastic volatility model, with dynamics as in Eq. (1), with risk premium $\gamma^* = -1/2$. The RV is a HARGL process, featuring a transition density given by a non-central gamma, with parameters β^*, δ^*, c^*.*

Therefore, in the implementation of the model for option pricing, ν_1 is the unique parameter to be calibrated. All the other parameters can be computed explicitly in closed-form, once ν_1 has been calibrated. In Section 4.2., we provide the guidelines for the calibration of ν_1.

3. Estimation: methodology and diagnostics

In this section we provide the estimation methodology for the HARG family of models introduced in the previous section. Then, we analyze the dynamic properties of the proposed models under

the historical ($\mathbb{P}$) measure. For the sake of completeness, we compare the HARG family's features with those of several competitor models. Specifically, we consider an extension of the the Heston and Nandi (2000) GARCH(1,1) model and the Christoffersen, Jacobs, Ornthanalai, and Wang (2008) Two-Component GARCH(1,1) model, and the restricted models HARG, ARGL, and ARG .

3.1. Competitor models

The HARGL is a discrete-time model relying on historical observations. Thus, the first natural competitors come from the class of GARCH-type option pricing models. In particular, the first GARCH-type model we consider here is the widely applied GARCH(1,1) option pricing model, proposed by Heston and Nandi (2000) (GARCH hereafter). The Heston and Nandi model is an asymmetric GARCH in which the log-return and conditional variance under $\mathbb{P}$ are modelled by

$$\begin{aligned} y_{t+1} &= r + \lambda h_{t+1} + \sqrt{h_{t+1}} z_{t+1}, \\ h_{t+1} &= w + b h_t + a(z_t - c\sqrt{h_t})^2, \end{aligned} \tag{13}$$

with $z_{t+1} \sim N(0,1)$. In the conditional variance h_{t+1}, the parameter c captures the negative relation between shocks in the returns and volatility. The original model proposed by Heston and Nandi (2000) implies a SDF that comprises only compensation for equity risk while the SDF of the HARG family has additional compensation for variance risk. We thus consider a recent extension of the GARCH model developed by Christoffersen, Jacobs, and Heston (2011) where the standard SDF is augmented to include an independent variance risk compensation.[6] Specifically, the SDF considered in Christoffersen, Jacobs, and Heston (2011) can be written (see Appendix A4.) as:[7]

$$M_{t,t+1} = \frac{\exp(\phi y_{t+1} + \xi h_{t+2})}{\mathbb{E}_t^{\mathbb{P}}[\exp(\phi y_{t+1} + \xi h_{t+2})]}, \tag{14}$$

which is then comparable to Eq. (11); The free parameter ξ is calibrated on option prices.

The GARCH process represents a first attempt to model the non-constant volatility process; it is well-known that it fails to capture the strong persistence and the volatility of the volatility (see,

[6] In the usual GARCH framework the variance risk premium is generated through the equity risk premium parameter λ such that the two risk-premia are not independent.

[7] All the technical details about the risk-neutralisation of the Heston and Nandi GARCH with the aforementioned SDF can be found in Christoffersen, Jacobs, and Heston (2011).

e.g., Christoffersen, Jacobs, Ornthanalai, and Wang (2008)). Thus, to overcome this problem, the two-component GARCH (in the following, CGARCH) has been introduced recently. The second GARCH–type model we consider as a benchmark is then the CGARCH, whose conditional variance equation is given by

$$\begin{aligned} h_{t+1} &= q_{t+1} + b_s(h_t - q_t) + a_s((z_t - c_s\sqrt{h_t})^2 - (1 + c_s^2 q_t)), \\ q_{t+1} &= \omega + b_l q_t + a_l((z_t^2 - 1) - 2c_l\sqrt{h_t}z_t), \end{aligned} \tag{15}$$

where $(h_t - q_t)$ and q_t represent the short and long-run persistent components, respectively. As the component model of Engle and Lee (1999), the CGARCH model is the combination of two variance factors, which gives rise to a GARCH process with a more persistent dynamics than the standard one. Christoffersen, Jacobs, Ornthanalai, and Wang (2008) show that the CGARCH is successful in option pricing, since the long-memory plays a crucial role in the price of medium/long-maturity ATM options. For the CGARCH a suitable SDF with independent variance compensation is not available and its development is beyond the scope of the present paper. To overcome the problem of a possible unfair comparison among the considered models, we fit the parameter ω under the risk-neutral distribution on option prices, thus substantially introducing a free parameter that helps the model in reconciling objective and risk-neutral dynamics. A comparison between the two persistent CGARCH and HARG(L) models is instructive in gauging the improvements due to both the stochastic volatility model specification (with leverage) and the use of RV.

Additional insights into the features of the HARGL model can be obtained by evaluating the gains due to both the leverage effect and the multi-components specification, netting out the effect of the RV. To this end, a comparison between the HARGL and the HARG illustrates the importance of the leverage L_t, while a comparison between the HARG and the ARG, which is the exact discrete-time version of the CIR process, illustrates the importance of a multi-component structure in stochastic volatility option pricing models.

3.2. Volatility measure and estimation methodology

One of the main advantages of our modeling is related to the estimation of the parameters characterizing our family of volatility processes (i.e., ARG, ARGL, HARG, and HARGL). For this family

of stochastic volatility models, we employ the RV computed from tick-by-tick data for the S&P 500 Futures, from January 1, 1990 to December 31, 2007.

We estimate the continuous component of the RV through the following three steps: (i) estimate the total variation of the log-price process using the tick-by-tick Two-Scales estimator proposed by Zhang et al. (2005) (with a fast scale of two ticks and a slower one of 20 ticks); (ii) purify the Two-Scales estimator from the jump component in returns by the Threshold Bipower variation method recently introduced in Corsi et al. (2010) with a significance level of 99%; (iii) remove the most extreme observations in the volatility series, seemingly due to volatility jumps (a feature not embedded in our model), employing a threshold-based jumps detection method: we set a four standard deviations threshold computed on a rolling window of 200 days. This procedure affects about 1.5% of the observations in our sample. A further additional care is needed. The RV is a measure of the integrated variance during the trading period, i.e. from open to close. As a result, it neglects the contribution coming from overnight returns. To overcome this problem, we rescale our RV estimator to match the unconditional mean of the squared daily (i.e., close-to-close) returns. We label the resulting RV measure as Continuous Realized Volatility (CRV).[8]

Thanks to the use of the RV as a proxy for the unobservable volatility, we can simply estimate the parameters of the family of stochastic volatility processes using the Maximum Likelihood Estimator[9] on observable historical data. For the model specified in Eq. (7), the conditional transition density is available in closed-form (see Gourieroux and Jasiak 2006) so that the log-likelihood has the following series-expansion:

$$l_t^T(\theta) = -\sum_{t=1}^{T} \frac{1}{c}(RV_t + c\beta'(\mathbf{RV_{t-1}}, L_{t-1}) + \sum_{t=1}^{T} \log\left\{\sum_{k=1}^{\infty} \frac{RV_t^{\delta+k-1}}{c^{\delta+k}\Gamma(\delta+k)} \frac{[\beta'(\mathbf{RV_t}, L_{t-1})]^k}{k!}\right\}, \qquad (16)$$

where $\theta := (\delta, \beta', c)$.

The log-likelihood in Eq. (16) cannot be applied directly since it contains an infinite number of terms. Thus, to implement the Maximum Likelihood Estimator, we need to truncate the infinite sum in Eq. (16) to the $\varkappa$-th order. The tuning parameter $\varkappa$ can be selected using the AIC or the BIC or by simply looking at the stability of the estimates for different $\varkappa$ values. In our implementation, we

[8] To keep the discussion as more general as possible we will use interchangeably RV and CRV in the reminder of the paper and we will make clear the precise measure used whenever relevant.

[9] See Gourieroux and Jasiak (2006) for a related discussion.

set $\varkappa = 90$, since we noticed that larger values of $\varkappa$ imply neither any significant improvement in the accuracy of the approximation nor any change in the estimates.

To estimate the market price of risk $\tilde{\gamma}$ in the log-return equation, we apply the following simple regression model to the cum-dividend log-return:

$$y_{t+1} = r + \left(\tilde{\gamma} - \frac{1}{2}\right) RV_{t+1} + \sqrt{RV_{t+1}}\epsilon_{t+1}. \tag{17}$$

This equation can be re-written as

$$\begin{aligned} \frac{y_{t+1} - r + \frac{1}{2}RV_{t+1}}{\sqrt{RV_{t+1}}} &= \tilde{\gamma}\sqrt{RV_{t+1}} + \epsilon_{t+1}, \\ \tilde{y}_{t+1} &= \tilde{\gamma}\sqrt{RV_{t+1}} + \epsilon_{t+1}. \end{aligned} \tag{18}$$

Since $\epsilon_{t+1}|RV_{t+1}$ is assumed $N(0,1)$, the estimation and testing for the model in Eq. (18) both can be achieved by customary methods. Specifically, the FED Fund rate provides us with a proxy for the risk-free rate (r). Then, we estimate $\tilde{\gamma}$ by robust OLS,[10] obtaining an estimated value of 0.51, with a significant t-statistics (about 26).

As is customary in the literature, the GARCH-type models' parameters are estimated using the Maximum Likelihood Estimator, with Gaussian innovation distribution. The conditional variance is provided in Eq. (13) or Eq. (15).

In Table 1, we show the estimated parameters, their standard deviations, and the value of the likelihood function for the HARGL and GARCH families, respectively.

[Table 1 should be here]

For the HARGL model, the impact of past lags on the present value of RV is given by the partial autocorrelation coefficients, $c\beta'$. According to our estimates (considering also the leverage effect L_t), the sensitivity of RV_t on the conditional mean of RV_{t+1} is $c(\beta_1 + \beta_4/2) = 0.41$, whereas the sensitivity of RV_t^w and RV_t^m are $c\beta_2 = 0.31$ and $c\beta_3 = 0.12$, respectively. We notice that, for each model, the RV coefficients are all significant and show a decreasing impact of the past lags on the present value of the RV. This is in line with the literature; see Corsi (2009). Moreover, comparing the log-likelihood of

[10] Given the normality assumption of $\epsilon_{t+1}|RV_{t+1}$ the OLS estimator coincides with MLE. Robust OLS is a modified version of the OLS aimed to yield estimates which are less sensitive to the presence of outliers; see, e.g., Hampel, Ronchetti, Rousseeuw, and Stahel (2005).

the three RV models, we notice that the inclusion of both multiple factors (HARG) and the leverage component (HARGL) improves upon the value of the likelihood of the competitor models.[11]

3.3. Diagnostics and goodness-of-fit: conditional dynamics for volatility

We here analyze the dynamic properties of our RV based stochastic volatility models. The goal of this section is to study the ability of each model to replicate the observed conditional dynamics features of the RV. To this end, for each member belonging to our class of stochastic volatility models, we compute some diagnostics of the quality of fit of the transition distribution. Since we are analysing the transition distribution function, our goodness-of-fit diagnostics implicitly consider the ability of each model to fit all the conditional moments of the RV. For the sake of brevity, we here describe the results only for the models including the leverage effect (namely, HARGL and ARGL). Similar conclusions are obtained also for the models without leverage (namely, HARG and ARG).

Our analysis relies on the methodology proposed by Diebold et al. (1998) and Bates (2000). Let us label rv_t, for $t = 1, ..., T$, the observations of the RV. For each model, we compute the transition distribution function $\tilde{z}_t := P_{RV}(RV_t \leq \mathrm{rv}_t | \mathcal{F}_{t-1}, \hat{\theta})$, where $\hat{\theta}$ represents the Maximum Likelihood Estimator for the parameter θ in the considered realized volatility model. If the transition distribution is correctly specified with correct parameters, the $\tilde{z}_t$ are independent and identically distributed, with an uniform distribution $\mathcal{U}(0,1)$. Following Bates (2000), we apply a monotone transformation to $\tilde{z}_t$, defining $z_t = N^{-1}(\tilde{z}_t)$, where $N^{-1}(\cdot)$ is the inverse Cumulative Distribution Function of a $N(0,1)$. Under correct model specification, z_t should be independent and identically distributed draws from a $N(0,1)$. Conversely, if the conditional distribution is misspecified, the analysis of z_t detects the overall misspecification of the conditional density.

[Figure 2 should be here]

In Fig. 2, we analyze the distribution of z_t, comparing it to the $N(0,1)$. We notice that the HARGL is successful in centring the distribution and capturing a large part of the central probability mass. Indeed, the twenty-fifth quantile (Q25) and seventy-fifth quantile (Q75) of a standard normal

[11] The log-likelihood of the RV models and that of the GARCH-type models are clearly not comparable, an incompatibility arising from two different sets of data (RV and daily returns).

are about -0.67 and 0.67, respectively, and the HARGL implies that Q25 is -0.75 and Q75 is 0.8. Analogous considerations hold for the ARGL process (right top panel), which has values of Q25 (-0.67) and Q75 (1.02). The quantiles and other summary statistics for all the considered models are shown in Table 2.

[Table 2 should be here]

The wider quantile difference (Q75-Q25) highlights that neither the HARGL nor the ARGL are able to capture completely the actual transition density. This feature is illustrated in the top left (HARGL) and right (ARGL) panels of Fig. 2. For both the HARGL and ARGL processes, the Shapiro-Wilks test does not accept the assumed $N(0,1)$ distribution for z_t. Given that our sample contains almost 5,000 observations, the rejection of the $N(0,1)$ assumption is not surprising, since the test is very close to having trivial power. Nevertheless, looking at Table 2, we do remark that the values of skewness and kurtosis are quite similar to their counterparts in the standard normal.

We supplement our investigation with a graphical analysis of the Sample Auto-Correlation Function (SACF) of z_t and of its higher order moments: $(z_t - \bar{z})^\alpha$, for $1 \leq \alpha \leq 4$. According to Diebold et al. (1998), the SACF of the higher moments of z_t can provide useful information about the deficiencies of the higher-moments forecasts. Specifically, the existence of dependence in the correlogram of $(z_t - \bar{z})$,$(z_t - \bar{z})^2$,$(z_t - \bar{z})^3$, and $(z_t - \bar{z})^4$ reveals misspecification in the conditional mean, conditional variance, conditional skewness, and conditional kurtosis, respectively. Fig. 2 shows the SACFs for the previous quantities for the HARGL and ARGL models. All the SACF show some dependence patterns, a feature indicating deficiencies of the transition dynamics fitting. However, the SACF of every power transformation of $(z_t - \bar{z})$ of the HARGL is smaller than the corresponding SACF of the ARGL. Moreover, unreported results confirm that every SACF of the HARG is larger than every corresponding SACF of the HARGL, while every SACF of the ARG is larger than every corresponding SACF of the ARGL.

We conclude that the HARGL has the smallest model misspecification among the stochastic volatility models considered in our analysis. This implies that the HARGL is the model yielding the best fit of the transition distribution. This superior performance under the physical measure $\mathbb{P}$ will also be reflected in good pricing performances under the martingale measure $\mathbb{Q}$. This aspect will be investigated in the next section.

4. Option pricing: performance assessment

4.1. Data description

In this section, we describe the data employed in our empirical analysis. We use European options, written on the S&P 500 index. The observations for the option prices range from January 1, 1996 to December 31, 2004, and the data[12] are downloaded from OptionMetrics. Following Barone-Adesi, Engle, and Mancini (2008), options with time to maturity less than 10 days or more than 360 days, implied volatility larger than 70%, or prices less than 0.05 dollars are discarded. Moreover, we consider only out-of-the-money (OTM) put and call options for each Wednesday, which tend to be more liquid. This procedure yields a total number of $39,215$ observations. The numbers of put and call options are approximately the same, since we have about 51% put and 49% call options.

To perform our analysis, we split the options into different categories, classifying them according to either time to maturity or moneyness. In particular, we use K/S_t as a measure of moneyness. In our empirical application, a put option is said to be Deep OTM (DOTM hereafter) if $m \leq 0.94$ and OTM if $0.94 < m \leq 0.96$. A call option is said to be DOTM if $m \geq 1.04$ and OTM if $1.02 < m \leq 1.04$.. According to maturity τ, we classify options as short-maturity ($\tau < 60$ days), medium maturity (τ between $60 - 160$ days), and long maturity ($\tau > 160$ days).

[Table 3 should be here]

Considering the IV values reported in Table 3, the data show a strong volatility smile/smirk for both short- and long-maturity options. This implies that the risk-neutral distribution of the log-return is far from Gaussian, even after one year, suggesting that a persistent, either time-varying or stochastic volatility model needs to be applied to address these features.

4.2. Option pricing method

In Section 2.1.3., we derive the one-step-ahead LT of the joint process K'_{t+1}, see Eq. (8). For any given maturity, the computation of the multi-step-ahead conditional LT of the (H)ARG model can

[12] OptionMetrics also provides the Zero-Coupon yield curve and the Index dividend yield that we use in the pricing procedure.

be obtained in an analogous way: solving a system of recursive equations and thus obtaining a semi-closed-form expression for the option price. For long-maturities, the solving of this system of equations is computationally demanding. Therefore, we prefer to simplify the pricing procedure, applying a straightforward Monte Carlo simulation method to all RV option pricing models of the HARG family. In fact, one additional feature of our class of models is that both the sample paths of the log-return and of the RV can be easily simulated.Thus, we obtain the option prices for our class of models using the following four steps: (i) estimation under the physical measure $\mathbb{P}$; (ii) unconditional calibration of the parameter ν_1 such that the model-generated IV for an ATM one-year-maturity option (the longest maturity in our sample) matches the average market IV for the same maturity;[13] (iii) mapping of the parameters of the model estimated under $\mathbb{P}$ into the parameters under $\mathbb{Q}$ to specify the dynamics of the RV and the log-return under the martingale measure $\mathbb{Q}$ using Corollary 4; and (iv) for every t, simulation of both the RV and log-return $\mathbb{Q}$-dynamics so that, for each maturity τ and strike K, we compute the prices for call OTM options at time t as the average, $(1/L)\exp^{-r\tau}\sum_{l=1}^{L}\max(S_\tau^{(l)}-K,0)$. In the previous formula, L represents the total number of Monte Carlo simulations. In our numerical analysis, we set $L=50,000$.

For the GARCH and CGARCH models (since the MGF coefficients are quicker to compute) we have computed option prices using the Fourier-cosine series expansion method described in Fang and Oosterlee (2008), which has been proven to be both fast and reliable.

[13]The purpose of the calibration is the selection of ν_1 such that the model-unconditional volatility under the risk-neutral measure matches the unconditional risk-neutral volatility. Given that we do not directly observe the latter, we use the market-observed IV as an instrument to be matched with the model-generated IV, since they both depend directly on the volatility under the risk-neutral measure. Alternatively, we could have constructed a model-free expected risk-neutral volatility (analogously to the VIX index), using long-term options, and calibrated ν_1 to match its unconditional mean, for example. We prefer the first method, since the small number of long-maturity options, and their scarce liquidity, could both potentially affect the reliability of the computed risk-neutral expected volatility, leading to a possibly biased estimation of the unconditional expectation.

4.3. Option pricing results

4.3.1. Static properties

As is customary in the literature, we here analyze the option pricing performances of each model in terms of Root Mean Square Error on prices ($RMSE_P$) and on the percentage IV ($RMSE_{IV}$). The former emphasizes the importance of ATM options, which are the most expensive, while the latter tends to put more weight on OTM options.[14] In Table 4, we show the static performances.

[Table 4 about here]

The first row shows the absolute $RMSE_{IV}$ and $RMSE_P$ for the HARGL, while the remaining rows display the HARGL relative performances with respect to other models. Specifically, we compute the ratio between the $RMSE$ of the HARGL and that of each competitor model. A value less than one indicates an outperformance of the HARGL model.[15]

At first glance, the HARGL outperforms all competitors, both in terms of $RMSE_{IV}$ and $RMSE_P$. A closer inspection shows that in terms of $RMSE_P$ ($RMSE_{IV}$), (i) the HARGL improves of about 14% (14%) over the HN GARCH; (ii) the HARGL outperforms the CGARCH by about 16% (7%); (iii) the HARGL improves on all its restricted model specifications.

To gain a deeper understanding of the pricing performances, Table 5 and Table 6 report the results in terms of both $RMSE_{IV}$ and $RMSE_P$, disaggregated for different maturities (τ) and moneyness (m). In both the tables, Panel A shows the RMSE of the HARGL model in absolute terms. The other panels display the relative performances.

[Table 5 about here]

Let us consider Table 5: Panel A shows that the HARGL implies some degree of under-pricing for DOTM put options. This is on the one hand, a common feature of stochastic volatility option pricing models without jumps, since they cannot completely capture the probability mass in the left

[14] See, e.g., Broadie, Chernov, and Johannes (2007) for a discussion of the $RMSE_{IV}$ properties and Christoffersen and Jacobs (2004) for some comments about the importance of the loss function in option pricing.

[15] The relative performances for all the models considered in this paper can be computed using the ratios displayed in Table 4.

tail of the volatility transition density (see Section 3.3.) and on the other hand related to our leverage specification as discussed in Section 2.1.2..

The general improvement of the HARGL with respect to the GARCH model is remarkable across moneyness and maturity (Panel B), particularly for ATM options. The reason is twofold: the direct use of RV helps in pricing short-term options, while the long-memory structure improves on the pricing of long-term options.

The improvements on the CGARCH are evident especially for short- and medium-term options (Panel C), whereas for long-term options the two model seems to produce very similar results, both being able to reproduce the persistence in volatility.

It is interesting to note that the GARCH out-performs the simple ARG model (Panel D). This result is mainly driven by a better pricing of the GARCH for short-maturity options. The reason of this apparently counterintuitive output is that the RV, although is a precise measure of daily variation, it is much noisier than the expected quadratic variation over the option maturity. The latter quantity is the main determinant of the option price. Indeed, as can be seen from Fig. 3, the RV is much noisier than the VIX. Since the ARG model uses only the first lag of the RV, it loads this noise on the option prices, yielding less accurate prices, while the GARCH smooths the noise by construction. In that sense, we argue that employing a multi-component model (such as the HARG/HARGL) not only provides the volatility process with the necessary persistence, but it also helps in smoothing the noise affecting the RV measure.

[Figure 3 about here]

By looking at the other panels, we disentangle the role that each ingredient in the HARGL model plays across different maturities and moneyness. Panel E reports the comparison between the full HARGL model and the simplest counterpart ARG, while in the other panels we disaggregate the improvements due to the long-memory and the leverage.

A comparison between the HARG and the ARG models (Panel F) and HARGL and ARGL (Panel G) confirms the importance of the heterogeneous multi-component specification. In particular, the persistence implied by the three RV components yields advantages in pricing ATM options with long-maturities (see the last two columns of Panel E).

The importance of the leverage effect is disentangled by looking at Panel H where the HARGL and HARG models are compared. We notice that for ATM options, the HARG model has a performance similar to that of the HARGL, since the two models share the same degree of persistence in the volatility term structure. However, the HARGL has a smaller $RMSE_{IV}$ on DOTM and OTM put options, thanks to the presence of the leverage component.

It is evident from this analysis that all the ingredients (RV, persistence and leverage) are necessary to accurately price options across different maturities and strikes. This is the reason why the HARGL consistently shows the best option pricing performance among the considered models. Analogous considerations hold in terms of $RMSE_P$ (see Table 6).

[Table 6 about here]

We conclude this section by analysing the performance of the option pricing models under different volatility regimes. To perform this analysis, we divide the sample period into three sub-samples: low and declining, medium and increasing, and high-volatility. The three different regimes have been identified using the volatility levels given by the VIX index, as shown in Fig. 3 (top panel). For comparison, Fig. 3 also displays the time evolution of the CRV series (bottom panel).

Fig. 4 compares the average IVs of near-ATM options observed in the data with the IVs obtained by the CGARCH, ARGL, and HARGL models. We analyze the three volatility periods separately.

[Figure 4 about here]

We notice that in the low- and medium-volatility regimes, the pricing of the HARGL is very precise for short- and medium-maturities, while it tends to underestimate the IV at longer maturities. However, from a joint analysis of the three panels of Fig. 4, the HARGL model shows a remarkable feature: it always appears very close to the market data, irrespective of the volatility regime.

4.3.2. Dynamic properties

In addition to the static analysis carried out in the previous section, we here investigate the ability of the different models to describe the dynamic evolution of the IV surface. Specifically, we first focus our attention on the overall pricing of ATM options through time and then disaggregate the results over the short- and long-ends of the IV surface.

Fig. 5 analyzes the dynamics of the ATM option bias for the different models. All the considered models appear to be unconditionally unbiased thus validating our unconditional model calibration methods. GARCH-type models show a significant variation in their pricing, while the HARGL produces a pricing error with the smallest standard deviation.

[Figure 5 about here]

Moreover, in order to study the model's ability to track the dynamics of the short-end of the IV surface, we show in Fig. 6 the evolution of the IV level (i.e. the average IV of short-term ATM options) implied by the CGARCH, GARCH, HARGL, and ARGL. Tracking the level is crucial for capturing the overall dynamics of the IV surface. We notice that both the CGARCH and the GARCH tend to reproduce the empirical level dynamics with some delay (especially during periods of increasing volatility). Incidentally, we notice that the delay is smaller in the very first part of the sample, which largely coincides with the observation period in Christoffersen, Jacobs, Ornthanalai, and Wang (2008), however, it becomes more pronounced in the rest of the sample. More reactive dynamics can be obtained by using stochastic volatility models based on RV. This is the case for both the HARGL and the ARGL. The two bottom panels highlight that the fast-adapting nature of the RV allows our class of models to adapt more rapidly to changes in market volatility. However, as can be seen form Fig. 3, the RV is noisier than the VIX. This implies that, if a simple autoregressive model of order one is employed, the noise is transmitted to option prices, as can be seen in the third panel of Fig. 6. On the contrary, the multi-component specification of the HARG(L) provide the necessary smoothing to deliver accurate volatility forecast and option prices. The HARGL thus produce the best performances, both qualitatively and quantitatively, exploiting the information contained in the data more thoroughly than the filtering procedure applied by GARCH-type models.

[Figure 6 should be here]

Finally, looking at the dynamics of the IV term-structure (i.e. the difference between the average IV of ATM long-maturity options and the level), as shown in Fig. 7, we clearly identify the benefit of combining a persistent model with the use of RV. The HARGL performs remarkably well, especially in the second part of the sample (i.e. from 2001 to 2007). The CGARCH is penalized since, as seen

in Panel A, it struggles to track the dynamics of the level while the GARCH still show some delay in adapting to market changes.

[Figure 7 should be here]

Summarising, the proposed HARGL model, in general, is able to reproduce closely both the IV level and term-structure dynamics, improving upon the considered GARCH-type models. The fast-adapting properties of the RV and the ability of the HARGL to generate a realistic degree of persistence are both necessary ingredients that lead to an accurate modeling of the evolution of the ATM-IV surface over time.[16]

4.4. Risk-premia interpretation

The SDF proposed in Eq. (11) implies the compensation for two sources of risk: one is related to shocks in the log-return and the other concerns the stochastic volatility. The risk-premium coefficients (ν_2 and ν_1) have the following interpretation.

As far as ν_2 is concerned, from the proof of Proposition 3 (see Appendix A), we have $\nu_2 = \gamma + 0.5 = \tilde{\gamma}$. From Eq. (1) and Eq. (2), we notice that $\tilde{\gamma}$ represents the market risk premium. Thus, there is a one-to-one relation between the parameter ν_2 in the SDF and the market risk-premium in the log-return equation. Interestingly, this feature is analogous to the standard risk compensation adopted in the GARCH literature (see, e.g., Duan 1995). This similarity is related to two important features of our model. First, as in the GARCH formulation, the risk-premium γRV_{t+1} is an affine function of the state variable (see Eq. (17)). Second, the one-day-ahead transition density of the log-return, given the current level of the volatility, is Gaussian (see Eq. (7)). The latter feature is standard in the GARCH literature.[17]

As far as ν_1 is concerned, we remark that in Eq. (11), it multiplies RV_{t+1}. However, the compensation for the volatility risk is not simply represented by ν_1. From an inspection of the log-return

[16] Unreported results show that HARG-HARGL and ARG-ARGL models have markedly similar performances in the evolution of ATM bias, IV level, and term-structure. This is related to the fact that the leverage effect has a negligible impact on pricing the ATM options.

[17] See, e.g., Assumption 1 in Heston and Nandi (2000) or, more generally, Christoffersen, Jacobs, and Ornthanalai (2008), for the class of GARCH models assuming a normal transition density for the log-return dynamics.

specification, we notice that the RV_{t+1} has effects on the conditional mean and the conditional variance of y_{t+1}. Since the latter is multiplied in the SDF by ν_2, the compensation for the risk due to RV_{t+1} relies on a combination of ν_2 and ν_1. Specifically, if we set $\nu_1 = 0.5\,\nu_2(\nu_2 - \gamma)$, we remove the compensation for the volatility risk. This can be easily seen from the proof of Proposition 3 in Appendix A, Eq. (24). Indeed, straightforward calculations show that λ in Proposition 3 becomes identically zero. Thus, there is no change of measure for the volatility process: the dynamics of RV is identical under the physical and risk-neutral measure.

The pricing performance in the special case in which there is no compensation for the volatility risk (i.e. $\nu_1 = 0.5\,\nu_2(\nu_2 - \gamma)$) deteriorates significantly, for every model belonging to the HARG family. For instance, in the case of the HARGL model, the $RMSE_{IV}$ and $RMSE_P$ are equal to 6.485% and 0.011, respectively. This implies that, at least for the period covered by our sample and given our model specification, taking into account compensation for volatility risk is essential. The effect of doing so is twofold: (i) it helps to match the long-term IV, and (ii) it affects the persistence of the RV dynamics, giving an additional degree of freedom to fit the IV term structure. The presence of a substantial (negative) variance risk premium (especially in the S&P 500 Index) has been previously documented in the literature for example by Bakshi and Kapadia (2003) and Carr and Wu (2009).

4.5. Robustness to sample period and RV measures

In this final section we check the robustness of the pricing results with respect to the use of different RV measures and to the presence of extreme events in the estimation period of the models. Specifically, we consider three different RV measures: (i) the five minute return RV (RV5min); (ii) the Zhang et al. (2005) Two-Scale estimator (TS), and (iii) the RV measure employed in the previous sections, which is the continuous part of the TS measure (CRV), obtained as described in Section 3.2..

We also consider two different estimation periods. The first goes from 1985 to 2007 (including the 1987 crash and the frequent intradaily RV spikes during the 1987-1989 period (see Bates 2000), and the second goes from 1990 to 2007. A summary of the HARGL model's option pricing results is reported in Table 7 (the complete set of detailed results, for the different models over different maturity/moneyness bins, are available from the authors upon request).

As far as the estimation period is concerned, we notice that the overall performance remain stable

for the CRV case while it deteriorates for the other measures when the estimation period is extended to 1985. This is due to the turmoil in financial markets. The crash in 1987, the turmoil in October 1989, and the following crisis have determined features in the RV dynamics that are no longer representative of the stochastic behavior of the RV during the pricing period 1996-2004. This can be noticed, for instance, by analysing the volatility persistence over the period 1985-1990. Unreported computations highlight that the SACF of the TS and RV5min in the period 1985-1990 is much lower than the SACF from 1990-2007. This feature reduces the persistence of the estimated HARGL model, leading to the deterioration of the HARGL pricing performance over the 1996-2004 period. The jump detection techniques employed in the construction of the CRV measure instead lead to stable estimates and thus to similar pricing.

Conditional on a given time period, the variations in the performances among the three RV measures again underly the importance of extreme observation in the estimation of the HARGL. This can be seen particularly in the period 1985-2007, where the CRV measure shows considerably better pricing performance than the TS and RV5min, which both appear more sensitive to the presence of extreme events in the RV dynamics. Thus, we conclude that the CRV measure employed strikes the best balance between precision (during quiet periods) and robustness to extreme events (during more turbulent periods).

5. Conclusion

In this paper, we develop a discrete-time stochastic volatility option pricing model that exploits the historical information contained in the high-frequency data. Using the RV as a proxy for the unobservable returns volatility, we propose a long-memory process with a leverage effect: the HARGL process. Our model can be considered a reduced form, multi-components model, since it is characterized by three volatility components (or frequencies): short-, medium-, and long-horizon. Making the latent volatility observable (through the RV), the HARGL model can be easily estimated by using observed historical data. This is a clear advantage with respect to other stochastic volatility models, which rely on time-consuming filtering procedures. The $\mathbb{P}$- and $\mathbb{Q}$-dynamics are reconciled through the definition of an exponentially affine SDF, which takes into account for both equity and variance risk-premium. This leads to a tractable dynamics under the risk-neutral measure. The extensive empirical analysis

of the S&P 500 index options shows that two ingredients are crucial for option pricing performance: (i) the use of RV, which provides an accurate and fast-adapting proxy for the unobserved volatility, and (ii) the high persistence and necessary smoothing generated by the HARGL volatility model specification. Thanks to both these features, the HARGL is better able to reproduce the $\mathbb{Q}$-dynamics, hence, outperforming competing GARCH-type and other RV based stochastic volatility option pricing models (ARG, ARGL, and HARG).

A Techinical Appendix: Proofs

A1. Proof of Proposition 1

Proof. Let us compute

$$\begin{aligned}
\mathbb{E}_t^{\mathbb{P}}\left[\exp(-\alpha' K_{t+1})\right] &= \mathbb{E}_t^{\mathbb{P}}\left[\exp(-\alpha_1 RV_{t+1} - \alpha_2 y_{t+1})\right] \\
&= \mathbb{E}_t^{\mathbb{P}}\left[\exp(-\alpha_2\sqrt{RV_{t+1}}\varepsilon_{t+1} - (\alpha_1+\gamma\alpha_2)RV_{t+1})\right] \\
&= \mathbb{E}_t^{\mathbb{P}}\left[\exp\left(-\left(\alpha_1+\gamma\alpha_2-\frac{1}{2}\alpha_2^2\right)RV_{t+1}\right)\right] \\
&= \exp\left[-b\left(\alpha_1+\gamma\alpha_2-\frac{1}{2}\alpha_2^2\right) - a\left(\alpha_1+\gamma\alpha_2-\frac{1}{2}\alpha_2^2\right)\beta'(\mathbf{RV}_t, L_t)\right] \\
&= \varphi_K^{\mathbb{P}}(v), \qquad (19)
\end{aligned}$$

where $v := \alpha_1 + \alpha_2\gamma - \frac{1}{2}\alpha_2^2$. □

A2. Proof of Proposition 2

Proof. For the sake of simplicity, we assume a zero expected instantaneous rate of return ($r = 0$). Let

us first write the stochastic discount factor as

$$\begin{aligned} M_{t,t+1} &= \frac{\exp(-\nu_1 RV_{t+1} - \nu_2 y_{t+1})}{\mathbb{E}_t^{\mathbb{P}}\left[\exp(-\nu_1 RV_{t+1} - \nu_2 y_{t+1})\right]} \\ &= \frac{\exp(-\nu_1 RV_{t+1} - \nu_2 y_{t+1})}{\mathbb{E}_t^{\mathbb{P}}\left[\exp(-\nu_1 RV_{t+1})\mathbb{E}_t^{\mathbb{P}}[\exp(-\nu_2 y_{t+1})|RV_{t+1}]\right]} \\ &= \frac{\exp(-\nu_1 RV_{t+1} - \nu_2 y_{t+1})}{\mathbb{E}_t^{\mathbb{P}}\left[\exp(-\nu_1 RV_{t+1} - \nu_2\gamma RV_{t+1})\exp\left(\frac{RV_{t+1}\nu_2^2}{2}\right)\right]} \\ &= \frac{\exp(-\nu_1 RV_{t+1} - \nu_2 y_{t+1})}{\mathbb{E}_t^{\mathbb{P}}\left[\exp\left(-\left(\nu_1 + \nu_2\gamma - \frac{\nu_2^2}{2}\right)RV_{t+1}\right)\right]} \\ &= \frac{\exp(-\nu_1 RV_{t+1} - \nu_2 y_{t+1})}{\varphi_{RV}^{\mathbb{P}}(u)} \end{aligned} \tag{20}$$

where $u := \nu_1 + \nu_2\gamma - \nu_2^2/2$ and $\varphi_{RV}^{\mathbb{P}}(u)$ is the generic conditional LT of RV whose specific form depends on the model employed for the RV dynamics (ARG, ARGL, HARG, HARGL).

The no-arbitrage restrictions are

$$\mathbb{E}_t^{\mathbb{P}}\left[M_{t,t+1}\right] = 1 \tag{21}$$

$$\mathbb{E}_t^{\mathbb{P}}\left[M_{t,t+1}\exp(y_{t+1})\right] = 1. \tag{22}$$

The first condition is automatically satisfied. The second condition reads:

$$\begin{aligned} &\frac{1}{\varphi_{RV}^{\mathbb{P}}(u)}\mathbb{E}_t^{\mathbb{P}}\left[\exp(-\nu_1 RV_{t+1} - \nu_2 y_{t+1})\exp(y_{t+1})\right] \\ = &\frac{1}{\varphi_{RV}^{\mathbb{P}}(u)}\mathbb{E}_t^{\mathbb{P}}\left[\exp(-\nu_1 RV_{t+1} - (\nu_2 - 1)y_{t+1})\right] = 1. \end{aligned} \tag{23}$$

Using the moment generating function of y_{t+1}, the LHS of the Eq. (23) becomes:

$$\begin{aligned} &\frac{1}{\varphi_{RV}^{\mathbb{P}}(u)}\mathbb{E}_t^{\mathbb{P}}\left[\exp(-\nu_1 RV_{t+1})\mathbb{E}_t^{\mathbb{P}}[\exp(-(\nu_2 - 1)y_{t+1})|RV_{t+1}]\right] \\ = &\frac{1}{\varphi_{RV}^{\mathbb{P}}(u)}\mathbb{E}_t^{\mathbb{P}}\left[\exp(-\nu_1 RV_{t+1} - (\nu_2 - 1)\gamma RV_{t+1})\exp\left(\frac{RV_{t+1}(\nu_2 - 1)^2}{2}\right)\right] \\ = &\frac{1}{\varphi_{RV}^{\mathbb{P}}(u)}\mathbb{E}_t^{\mathbb{P}}\left[\exp\left(-\left(\nu_1 + (\nu_2 - 1)\gamma - \frac{(\nu_2 - 1)^2}{2}\right)RV_{t+1}\right)\right] \\ = &\frac{\varphi_{RV}^{\mathbb{P}}(\tilde{u})}{\varphi_{RV}^{\mathbb{P}}(u)} = 1 \end{aligned} \tag{24}$$

with $\tilde{u} := \left(\nu_1 + (\nu_2 - 1)\gamma - \frac{(\nu_2 - 1)^2}{2}\right)$. Therefore, in order to satisfy the no-arbitrage conditions we

need to have $u = \tilde{u}$, that is

$$\begin{aligned} \nu_2\gamma - \frac{\nu_2^2}{2} &= (\nu_2 - 1)\gamma - \frac{(\nu_2 - 1)^2}{2} \\ \nu_2 &= \gamma + \frac{1}{2}. \end{aligned} \tag{25}$$

□

A3. Proof of Proposition 3

Proof. Let us compute

$$\begin{aligned} & \mathbb{E}_t^{\mathbb{Q}}\left[\exp(-\alpha' K_{t+1})\right] = \mathbb{E}_t^{\mathbb{Q}}\left[\exp(-\alpha_1 RV_{t+1} - \alpha_2 y_{t+1})\right] \\ = \;& \mathbb{E}_t^{\mathbb{P}}\left[M_{t,t+1}\exp(-\alpha_1 RV_{t+1} - \alpha_2 y_{t+1})\right] \\ = \;& \frac{1}{\varphi_{RV}^{\mathbb{P}}(u)}\mathbb{E}_t^{\mathbb{P}}\left[\exp(-(\nu_1+\alpha_1)RV_{t+1})\mathbb{E}_t^{\mathbb{P}}[\exp(-(\nu_2+\alpha_2)y_{t+1})|RV_{t+1}]\right] \\ = \;& \frac{1}{\varphi_{RV}^{\mathbb{P}}(u)}\mathbb{E}_t^{\mathbb{P}}\left[\exp(-(\nu_1+\alpha_1)RV_{t+1} - (\nu_2+\alpha_2)\gamma RV_{t+1})\exp\left(\frac{RV_{t+1}(\nu_2+\alpha_2)^2}{2}\right)\right] \\ = \;& \frac{1}{\varphi_{RV}^{\mathbb{P}}(u)}\mathbb{E}_t^{\mathbb{P}}\left[\exp\left(-\left(\nu_1+\alpha_1+(\nu_2+\alpha_2)\gamma - \frac{(\nu_2+\alpha_2)^2}{2}\right)RV_{t+1}\right)\right] \\ = \;& \frac{\varphi_{RV}^{\mathbb{P}}(\varpi)}{\varphi_{RV}^{\mathbb{P}}(u)} \end{aligned} \tag{26}$$

with $\varpi := \nu_1 + \alpha_1 + (\nu_2+\alpha_2)\,\gamma - \frac{(\nu_2+\alpha_2)^2}{2}$. Considering the non-arbitrage conditions $\nu_2 = \gamma + \frac{1}{2}$ from Proposition 2, ϖ becomes

$$\begin{aligned} \varpi &= \nu_1 + \alpha_1 + (\nu_2+\alpha_2)\,\gamma - \frac{(\nu_2+\alpha_2)^2}{2} = \alpha_2(\gamma - \nu_2) + \alpha_1 - \frac{1}{2}\alpha_2^2 + \gamma\nu_2 + \nu_1 - \frac{\nu_2^2}{2} \\ &= -\frac{1}{2}\alpha_2 + \alpha_1 - \frac{1}{2}\alpha_2^2 + \nu_1 + \frac{\gamma^2}{2} - \frac{1}{8} \\ &= \zeta + \lambda \end{aligned} \tag{27}$$

where $\zeta := -\frac{1}{2}\alpha_2 + \alpha_1 - \frac{1}{2}\alpha_2^2$ and $\lambda := \nu_1 + \frac{\gamma^2}{2} - \frac{1}{8}$. We now specify the computation for the HARGL model, the others being particular cases of this:

$$\begin{aligned} &= \frac{\varphi_{RV}^{\mathbb{P}}(\zeta+\lambda)}{\varphi_{RV}^{\mathbb{P}}(\lambda)} \\ &= \frac{\exp\left(-b(\zeta+\lambda) - a(\zeta+\lambda)\beta'(\mathbf{RV}_t, L_t)\right)}{\exp\left(-b(\lambda) - a(\lambda)\beta'(\mathbf{RV}_t, L_t)\right)} \\ &= \exp\left(-\left[b(\zeta+\lambda) - b(\lambda)\right] - \left[a(\zeta+\lambda) - a(\lambda)\right]\beta'(\mathbf{RV}_t, L_t)\right). \end{aligned} \tag{28}$$

Thus

$$\mathbb{E}_t^{\mathbb{Q}}\left(\exp(-\alpha' K_{t+1})\right) = \exp\left(-b^*(\zeta) - a^*(\zeta)\left(\beta^{*\prime}(\mathbf{RV}_t, L_t)\right)\right), \tag{29}$$

in which $a^*(\zeta)$ and $b^*(\zeta)$ are such that

$$\begin{aligned} a^*(\zeta)\beta^* &= a(\zeta+\lambda)\beta - a(\lambda)\beta = \frac{c^*\beta^*\zeta}{1+c^*\zeta} \\ b^*(\zeta) &= b(\zeta+\lambda) - b(\lambda) = \delta^* \ln(1+c^*\zeta), \end{aligned} \tag{30}$$

where

$$\begin{aligned} \beta^* &= \frac{\beta}{1+c\lambda}, \\ \delta^* &= \delta, \\ c^* &= \frac{c}{1+c\lambda}. \end{aligned} \tag{31}$$

Moreover, a comparison between Eq. (29) and Eq. (19) shows that $\gamma^* = -\frac{1}{2}$. This concludes the proof.

□

A4. GARCH SDF

Proof. Following Christoffersen, Jacobs, and Heston (2011), the SDF used in the risk neutralization is assumed to be:

$$\frac{M_{t+1}}{M_t} = \left(\frac{S_{t+1}}{S_t}\right)^{\phi} \exp(\delta + \eta h_{t+1} + \xi(h_{t+2} - h_{t+1})), \tag{32}$$

where ϕ and δ govern the time preference, while η and ξ govern the respective aversion to equity and variance risk. From here, it easily follows that

$$M_{t,t+1} = \frac{M_{t+1}}{\mathbb{E}_t[M_{t+1}]} = \frac{M_t \exp(\phi y_{t+1} + \delta + \eta h_{t+1} + \xi(h_{t+2} - h_{t+1}))}{\mathbb{E}_t[M_{t+1}]}. \tag{33}$$

Taking out from the expectation operator all the measurable quantities (h_{t+1} is measurable with respect to the information available at time t), and after some algebra, we obtain:

$$\frac{M_{t+1}}{\mathbb{E}_t[M_{t+1}]} = \frac{\exp(\phi y_{t+1} + \xi h_{t+2})}{\mathbb{E}_t[\exp(\phi y_{t+1} + \xi h_{t+2})]}. \tag{34}$$

This concludes the proof. □

References

Adrian, T. and J. Rosenberg (2007). Stock returns and volatility: Pricing the long-run and short-run components of market risk. *Journal of Finance, forthcoming*.

Aït-Sahalia, Y. and L. Mancini (2008). Out of sample forecasts of quadratic variation. *Journal of Econometrics 147*(1), 17–33.

Andersen, T. G. and L. Benzoni (2010). Do bonds span volatility risk in the us treasury market? a specification test for affine term structure models. *The Journal of Finance 65*(2), 603–653.

Andersen, T. G., T. Bollerslev, and F. Diebold (2007). Roughing it up: Including jump components in the measurement, modeling and forecasting of return volatility. *Review of Economics and Statistics 89*, 701–720.

Andersen, T. G., T. Bollerslev, F. Diebold, and H. Ebens (2001). The distribution of stock returns volatilities. *Journal of Financial Economics 61*, 43–76.

Andersen, T. G., T. Bollerslev, F. Diebold, and P. Labys (2000). Great realizations. *Risk 13*(3), 105–108.

Andersen, T. G., T. Bollerslev, F. Diebold, and P. Labys (2001). The distribution of realized exchange rate volatility. *Journal of the American Statistical Association 96*, 42–55.

Andersen, T. G., T. Bollerslev, F. Diebold, and P. Labys (2003). Modeling and forecasting realized volatility. *Econometrica 71*, 579–625.

Andersen, T. G., T. Bollerslev, and D. Dobrev (2007). No-arbitrage semi-martingale restrictions for continuous-time volatility models subject to leverage effects, jumps and i.i.d. noise: Theory and testable distributional implications. *Journal of Financial Econometrics 138*(1), 125–180.

Andersen, T. G., T. Bollerslev, and X. Huang (2010). A reduced form framework for modeling volatility of speculative prices based on realized variation measures. *Journal of Econometrics*.

Ane, T. and H. Geman (2000). Order flow, trasaction clock, and normality of asset returns. *The Journal of Finance LV*, 2259–2284.

Bakshi, G. and N. Kapadia (2003). Delta-hedged gains and the negative market volatility risk premium. *Review of Financial Studies 16*(2), 527.

Barndorff-Nielsen, O., J. Kent, and M. Sorensen (1982). Normal variance-mean mixtures and z distribution. *International Statistical Review 50*, 145–159.

Barndorff-Nielsen, O. and N. Shephard (2002a). Econometric analysis of realized volatility and its use in estimating stochastic volatility models. *Journal of the Royal Statistical Society: Series B (Statistical Methodology) 64*, 253–280.

Barndorff-Nielsen, O. E. and N. Shephard (2001). Non-gaussian ornstein-uhlembech-based models and some of their rses in financial economics. *Journal of the Royal Statistical Society Series B*(63), 167–241.

Barndorff-Nielsen, O. E. and N. Shephard (2002b). Estimating quadratic variation using realized variance. *Journal of Applied Econometrics 17*, 457–477.

Barndorff-Nielsen, O. E. and N. Shephard (2005). How accurate is the asymptotic approximation to the distribution of realized volatility? In D. W. F. Andrews and J. H. Stock (Eds.), *Identification and Inference for Econometric Models. A Festschrift in Honour of T.J. Rothenberg*, pp. 306–331. Cambridge University Press.

Barone-Adesi, G., R. Engle, and L. Mancini (2008). A garch option pricing with filtered historical simulation. *Review of Financial Studies 21*, 1223–1258.

Bates, D. (2000). Post-'87 crash fears in the s&p 500 futures option market. *Journal of Econometrics 94*(1-2), 181–238.

Bertholon, H., A. Monfort, and F. Pegoraro (2008). Econometric asset pricing modelling. *Journal of Financial Econometrics 6*, 407–458.

Bollerslev, T. and O. H. Mikkelsen (1996). Modeling and pricing long memory in stock market volatility. *Journal of Econometrics 73*(1), 151–184.

Bollerslev, T., G. Tauchen, and H. Zhou (2009). Expected stock returns and variance risk premia. *Review of Financial Studies 22*(11), 4463.

Bollerslev, T. and V. Todorov (2011). Tails, fears and risk premia. *Journal of Finance, forthcoming*.

Broadie, M., M. Chernov, and M. Johannes (2007). Model specification and risk premia: evidence from futures options. *Journal of Finance 62*, 1453–1490.

Busch, T., B. Christensen, and M. Nielsen (2010). The role of implied volatility in forecasting future realized volatility and jumps in foreign exchange, stock, and bond markets. *Journal of Econometrics*.

Carr, P. and L. Wu (2004). The finite moment log stable process and option pricing. *The Journal of Finance LVIII*, 753–778.

Carr, P. and L. Wu (2009). Variance risk premiums. *Review of Financial Studies 22*, 1311–1341.

Christoffersen, P., B. Feunou, K. Jacobs, and N. Meddahi (2010). The economic value of realized volatility. Working paper.

Christoffersen, P. and K. Jacobs (2004). The importance of the loss function in option valuation. *Journal of Financial Economics 73*, 291–318.

Christoffersen, P., K. Jacobs, and S. Heston (2011, March). A carch option model with variance-dependent pricing kernel. working paper.

Christoffersen, P., K. Jacobs, and C. Ornthanalai (2008, November). Exploring time–varying jump intensities: Evidence from sp500 returns and options. Manuscript, McGill University.

Christoffersen, P., K. Jacobs, C. Ornthanalai, and Y. Wang (2008). Option valuation with long-run and short-run volatility components. *Journal of Financial Economics 90*(3), 272–297.

Clark, P. (1973). A subordinated stochastic process model with finite variance for speculative prices. *Econometrica 41*, 135–155.

Clements, M., A. Galvão, and J. Kim (2008). Quantile forecasts of daily exchange rate returns from forecasts of realized volatility. *Journal of Empirical Finance*. Forthcoming.

Comte, F., L. Coutin, and E. Renault (2003). Affine fractional stochastic volatility models with application to option pricing. *Preprint, university of Montreal*.

Comte, F. and E. Renault (1998). Long memory in continuous time stochastic volatility models. *Mathematical Finance 8*, 291–323.

Corsi, F. (2009). A simple approximate long-memory model of realized-volatility. *Journal of Financial Econometrics 7*, 174–196.

Corsi, F., D. Pirino, and R. Ren (2010). Threshold bipower variation and the impact of jumps on volatility forecasting. *Journal of Econometrics 159*(2), 276 – 288.

Cox, J. C., J. E. Ingersoll, and S. A. Ross (1985). A theory of the term structure of interest rates. *Econometrica 53*, 385–407.

Diebold, F., T. Gunther, and A. Tay (1998). Evaluating density forecasts, with applications to financial risk management. *International Economic Review 39*, 863–883.

Duan, J. C. (1995). The garch option pricing model. *Mathematical Finance 5*, 13–32.

Engle, R. and G. Gallo (2006). A multiple indicators model for volatility using intra-daily data. *Journal of Econometrics 131*(1-2), 3–27.

Engle, R. and G. Lee (1999). A permanent and transitory component model of stock return volatility, in ed. r. engle and h. white cointegration, causality, and forecasting: A festschrift in honor of clive wj granger.

Fang, F. and C. W. Oosterlee (2008). A novel pricing method for european options based on fourier-cosine series expansions. *SIAM Journal on Scientific Computing 31*, 826–848.

Gagliardini, P., C. Gouriéroux, and Renault (2011). Efficient derivative pricing by extended method of moments. *Econometrica Forthcoming*.

Gourieroux, C. and J. Jasiak (2006). Autoregressive gamma process. *Journal of Forecasting 25*, 129–152.

Gourieroux, C. and A. Monfort (2007). Econometric specification of stochastic discount factor models. *Journal of Econometrics 136*(2), 509–530.

Hampel, F., E. Ronchetti, P. Rousseeuw, and W. Stahel (2005). *Robust Statistics: The Approach Based on Influence Functions*. Wiley Series in Probability and Statistics.

Heston, S. and S. Nandi (2000). A closed-form garch option valuation model. *Review Financial Studies 13*(3), 585–625.

Li, G. and C. Zhang (2010). On the number of state variables in options pricing. *Management Science 56*(11), 2058.

Maheu, J. and T. McCurdy (2010). Do high-frequency measures of volatility improve forecasts of return distributions? *Journal of Econometrics*.

McAleer, M. and M. Medeiros (2008). A multiple regime smooth transition heterogeneous autoregressive model for long memory and asymmetries. *Journal of Econometrics 147*(1), 104–119.

Merton, R. C. (1980). On estimating the expected return on the market: an exploratory investigation. *Journal of Financial Economics 8*, 323–61.

Stentoft, L. (2008). Option pricing using realized volatility. Working Paper at CREATES, University of Copenhagen.

Zhang, L., Y. Aït-Sahalia, and P. A. Mykland (2005). A tale of two time scales: determining integrated volatility with noisy high frequency data. *Journal of the American Statistical Association 100*, 1394–1411.

	ARG	ARGL	HARG	HARGL		GARGH		CGARCH
Parameter					Parameter		Parameter	
$\tilde{\gamma}$			0.5215		λ	3.6091	λ	2.9392
			(0.02277)			(1.544)		(1.5614)
c	22.89	22.52	18.11	17.58	ω	2.857e-018	b_s	0.67044
	(0.201)	(0.2017)	(0.1601)	(0.1526)		(3.7603e-008)		(0.061499)
δ	1.764	1.642	1.358	1.395	b	0.88809	a_s	1.49e-006
	(0.03886)	(0.03976)	(0.04652)	(0.04739)		(0.0084516)		(6.5849e-007)
β_1	0.03318	0.03435	0.02513	0.01899	a	4.4595e-006	c_s	425.59
	(0.0003713)	(0.0003489)	(0.0003729)	(0.0006312)		(4.1813e-007)		(169.0385)
β_2	-	-	0.01556	0.01775	c	120.1969	ω	1.2667e-006
			(0.0003114)	(0.0006059)		(12.1024)		(1.8699e-007)
β_3	-	-	0.006425	0.007186			b_l	0.9861
			(0.0002796)	(0.0003798)				(0.0020844)
β_4	-	0.004093	-	0.008814			a_l	2.4502e-006
		(0.0005423)		(0.0007425)				(2.8226e-007)
							c_l	87.824
								(15.0899)
ν_1	0.1212	0.1226	0.122	0.1219	$(1-2a\xi)^{-1/2}$	1.115	$\hat{\omega}$	1.9237e-006
Log-likelihood	-23647	-23656	-23360	-23294	Log-likelihood	12428		12473
Persistence	0.7596	0.8197	0.8532	0.8495	Persistence	0.95252		0.99542

Table 1: Maximum likelihood estimates, robust standard errors, and models performance. The historical data for the ARG, HARG, and HARGL models are given by the daily CRV computed on tick-by-tick data for the S&P500 Futures (see Section 3.). The estimation period ranges from the period 1990-2007. The last parameter of each column has been fitted on option prices.

Model	Q5	Q25	Median	Q75	Q95	Mean	Std Dev	Skw	Kurt	SW P-value
ARG	-1.64	-0.58	0.17	1.02	2.38	0.24	1.22	0.17	3.13	0.00
ARGL	-1.82	-0.67	0.09	1.02	2.29	0.14	1.23	0.15	3.16	0.00
HARG	-1.82	-0.73	-0.02	0.80	2.26	0.07	1.23	0.25	3.22	0.00
HARGL	-1.83	-0.75	0.01	0.80	2.30	0.07	1.23	0.22	3.13	0.00

Table 2: Model misspecification tests. Fifth (Q5), twenty-fifth (Q25) quantiles, Median, seventy-fifth (Q75) and ninety-fifth (Q95) quantiles, and Mean, Standard Deviation (Std Dev), Skewness (Skw), and Kurtosis (Kurt) of $z_t = N^{-1}(P_{RV}(RV_t \leq \text{rv}_t|\mathcal{F}_{t-1}, \hat{\theta}))$, where $\hat{\theta}$ represents the Maximum Likelihood Estimator for the considered stochastic volatility model, as given in Table 1. The last column shows the P-values for the Shapiro-Wilks test.

	Maturity			
Moneyness	Less then 20	20 to 60	60 to 160	More then 160
	Implied volatility			
$m \leq 0.94$	0.2674	0.2446	0.2329	0.2325
$0.94 \leq m \leq 0.96$	0.2316	0.2242	0.2202	0.2246
$0.96 \leq m \leq 0.98$	0.2118	0.2110	0.2121	0.2190
$0.98 \leq m \leq 1.02$	0.1874	0.1954	0.2031	0.2120
$1.02 \leq m \leq 1.04$	0.1705	0.1803	0.1925	0.2041
$1.04 \leq m$	0.1833	0.1751	0.1835	0.1963
	Implied volatility standard deviation			
$m \leq 0.94$	0.0536	0.0525	0.0456	0.0433
$0.94 \leq m \leq 0.96$	0.0503	0.0505	0.0442	0.0425
$0.96 \leq m \leq 0.98$	0.0516	0.0486	0.0433	0.0420
$0.98 \leq m \leq 1.02$	0.0523	0.0484	0.0433	0.0425
$1.02 \leq m \leq 1.04$	0.0478	0.0466	0.0426	0.0439
$1.04 \leq m$	0.0444	0.0456	0.0403	0.0405
	Number of observations			
$m \leq 0.94$	1428	2596	1968	1201
$0.94 \leq m \leq 0.96$	874	1513	1005	597
$0.96 \leq m \leq 0.98$	1011	1752	1039	599
$0.98 \leq m \leq 1.02$	2180	3851	2122	1213
$1.02 \leq m \leq 1.04$	1022	1680	1049	543
$1.04 \leq m$	1987	3522	2735	1728

Table 3: Database description. Means and standard deviations of prices and implied volatilities of S&P 500 index out-of-the-money options on each Wednesday from January 1, 1996 to December 31, 2004 (39,215 observations) sorted by moneyness and maturity categories. Implied volatility is the Black-Scholes implied volatility. Moneyness is defined as $m = K/S_t$, where K and S are the strike and underlying price, respectively. Maturity is measured in calendar days.

	Performance measures	
Models	$RMSE_{IV}$	$RMSE_p$
HARGL	3.817	0.005
HARGL/GARCH	0.853	0.857
HARGL/CGARCH	0.735	0.923
ARGL/GARCH	0.990	1.093
HARGL/ARG	0.820	0.762
HARG/ARG	0.883	0.798
HARGL/ARGL	0.862	0.784
HARGL/HARG	0.928	0.955

Table 4: Global option pricing performance on S&P500 out-of-the-money options from January 1, 1996 to December 31, 2004, computed with the CRV measure estimated from 1990 to 2007. We use the maximum likelihood parameter estimates from Table 1. First row: percentage implied volatility root mean squared error ($RMSE_{IV}$) and percentage price root mean squared error ($RMSE_p$) of the HARGL model. Second and subsequent rows: $RMSE_{IV}$ and $RMSE_p$ of the benchmark models relative to the HARGL. Maturity is in days and moneyness $m = K/S_t$, where K and S are the strike and underlying price, respectively.

	Maturity			
Moneyness	$\tau \leq 20$	$20 < \tau \leq 60$	$60 < \tau \leq 160$	$160 < \tau$
Panel A	HARGL Implied Volatility RMSE			
$m < 0.94$	6.711	4.909	4.320	4.044
$0.94 < m \leq 0.96$	4.551	3.789	3.638	3.466
$0.96 < m \leq 0.98$	3.518	3.305	3.344	3.542
$0.98 < m \leq 1.02$	2.681	2.866	3.100	3.360
$1.02 < m \leq 1.04$	2.740	2.622	2.945	3.170
$1.04 < m$	3.143	2.698	2.996	3.194
Panel B	HARGL/GARCH Implied Volatility RMSE			
$m < 0.94$	0.879	1.132	0.993	0.937
$0.94 < m \leq 0.96$	1.034	0.973	0.898	0.888
$0.96 < m \leq 0.98$	0.919	0.915	0.859	0.877
$0.98 < m \leq 1.02$	0.778	0.801	0.799	0.829
$1.02 < m \leq 1.04$	0.836	0.716	0.752	0.804
$1.04 < m$	0.654	0.779	0.790	0.840
Panel C	HARGL/CGARCH Implied Volatility RMSE			
$m < 0.94$	0.689	0.910	0.983	1.073
$0.94 < m \leq 0.96$	0.778	0.850	0.958	1.037
$0.96 < m \leq 0.98$	0.677	0.840	0.954	1.028
$0.98 < m \leq 1.02$	0.677	0.810	0.940	0.994
$1.02 < m \leq 1.04$	0.900	0.866	0.967	0.982
$1.04 < m$	0.544	1.026	1.080	1.017
Panel D	ARGL/GARCH Implied Volatility RMSE			
$m < 0.94$	0.810	1.216	1.151	1.119
$0.94 < m \leq 0.96$	1.075	1.156	1.103	1.077
$0.96 < m \leq 0.98$	1.074	1.134	1.081	1.061
$0.98 < m \leq 1.02$	1.074	1.114	1.053	1.037
$1.02 < m \leq 1.04$	1.200	1.110	1.056	1.035
$1.04 < m$	0.860	1.194	1.083	1.042

	Maturity			
Moneyness	$\tau \leq 20$	$20 < \tau \leq 60$	$60 < \tau \leq 160$	$160 < \tau$
Panel E	HARGL/ARG Implied Volatility RMSE			
$m < 0.94$	0.998	0.894	0.850	0.835
$0.94 < m \leq 0.96$	0.904	0.822	0.808	0.824
$0.96 < m \leq 0.98$	0.821	0.793	0.791	0.826
$0.98 < m \leq 1.02$	0.704	0.705	0.751	0.796
$1.02 < m \leq 1.04$	0.662	0.618	0.696	0.771
$1.04 < m$	0.707	0.607	0.694	0.781
Panel F	HARG/ARG Implied Volatility RMSE			
$m < 0.94$	1.111	0.975	0.910	0.878
$0.94 < m \leq 0.96$	0.998	0.882	0.848	0.851
$0.96 < m \leq 0.98$	0.889	0.834	0.820	0.849
$0.98 < m \leq 1.02$	0.720	0.723	0.768	0.815
$1.02 < m \leq 1.04$	0.676	0.633	0.715	0.792
$1.04 < m$	0.749	0.651	0.736	0.820
Panel G	HARGL/ARGL Implied Volatility RMSE			
$m < 0.94$	1.085	0.931	0.863	0.837
$0.94 < m \leq 0.96$	0.962	0.842	0.814	0.824
$0.96 < m \leq 0.98$	0.856	0.807	0.795	0.827
$0.98 < m \leq 1.02$	0.724	0.720	0.759	0.799
$1.02 < m \leq 1.04$	0.697	0.645	0.712	0.777
$1.04 < m$	0.760	0.653	0.730	0.806
Panel H	HARGL/HARG Implied Volatility RMSE			
$m < 0.94$	0.898	0.917	0.934	0.950
$0.94 < m \leq 0.96$	0.906	0.932	0.953	0.968
$0.96 < m \leq 0.98$	0.924	0.951	0.964	0.973
$0.98 < m \leq 1.02$	0.977	0.975	0.977	0.978
$1.02 < m \leq 1.04$	0.980	0.977	0.973	0.973
$1.04 < m$	0.944	0.933	0.944	0.952

Table 5: Option pricing performance on S&P500 out-of-the-money options from January 1, 1996 to December 31, 2004, computed with the CRV measure estimated from 1990 to 2007. We use the maximum likelihood parameter estimates from Table 1. Panel A: percentage implied volatility root mean squared error ($RMSE_{IV}$) of the HARGL model sorted by moneyness and maturity. Panels B to H: $RMSE_{IV}$ of the benchmark models relative to the HARGL sorted by moneyness and maturity. Maturity is in days and moneyness $m = K/S_t$, where K and S are the strike and underlying price, respectively.

	Maturity			
Moneyness	$\tau \leq 20$	$20 < \tau \leq 60$	$60 < \tau \leq 160$	$160 < \tau$
Panel A		HARGL Price RMSE		
$m < 0.94$	0.004	0.007	0.009	0.011
$0.94 < m \leq 0.96$	0.004	0.006	0.008	0.010
$0.96 < m \leq 0.98$	0.004	0.006	0.008	0.011
$0.98 < m \leq 1.02$	0.003	0.005	0.008	0.011
$1.02 < m \leq 1.04$	0.003	0.005	0.008	0.011
$1.04 < m$	0.002	0.004	0.008	0.011
Panel B		HARGL/GARCH Price RMSE		
$m < 0.94$	1.059	1.075	0.974	0.909
$0.94 < m \leq 0.96$	0.978	0.944	0.878	0.857
$0.96 < m \leq 0.98$	0.918	0.893	0.834	0.847
$0.98 < m \leq 1.02$	0.769	0.788	0.780	0.810
$1.02 < m \leq 1.04$	0.794	0.725	0.751	0.801
$1.04 < m$	0.933	0.784	0.796	0.850
Panel C		HARGL/CGARCH Price RMSE		
$m < 0.94$	0.859	0.909	0.991	1.068
$0.94 < m \leq 0.96$	0.784	0.853	0.966	1.026
$0.96 < m \leq 0.98$	0.738	0.848	0.965	1.010
$0.98 < m \leq 1.02$	0.699	0.829	0.959	0.983
$1.02 < m \leq 1.04$	0.878	0.895	0.987	0.972
$1.04 < m$	1.052	1.011	1.091	1.013
Panel D		ARGL/GARCH Price RMSE		
$m < 0.94$	1.149	1.204	1.145	1.108
$0.94 < m \leq 0.96$	1.128	1.156	1.098	1.057
$0.96 < m \leq 0.98$	1.123	1.136	1.071	1.039
$0.98 < m \leq 1.02$	1.089	1.116	1.044	1.018
$1.02 < m \leq 1.04$	1.171	1.114	1.050	1.022
$1.04 < m$	1.246	1.183	1.080	1.033

	Maturity			
Moneyness	$\tau \leq 20$	$20 < \tau \leq 60$	$60 < \tau \leq 160$	$160 < \tau$
Panel E		HARGL/ARG Price RMSE		
$m < 0.94$	0.871	0.863	0.839	0.817
$0.94 < m \leq 0.96$	0.827	0.799	0.794	0.809
$0.96 < m \leq 0.98$	0.789	0.773	0.773	0.812
$0.98 < m \leq 1.02$	0.684	0.691	0.736	0.788
$1.02 < m \leq 1.04$	0.642	0.623	0.696	0.772
$1.04 < m$	0.694	0.618	0.698	0.793
Panel F		HARG/ARG Price RMSE		
$m < 0.94$	0.943	0.934	0.896	0.859
$0.94 < m \leq 0.96$	0.896	0.856	0.832	0.832
$0.96 < m \leq 0.98$	0.841	0.812	0.800	0.832
$0.98 < m \leq 1.02$	0.698	0.708	0.753	0.806
$1.02 < m \leq 1.04$	0.652	0.638	0.717	0.797
$1.04 < m$	0.731	0.657	0.740	0.835
Panel G		HARGL/ARGL Price RMSE		
$m < 0.94$	0.922	0.893	0.851	0.820
$0.94 < m \leq 0.96$	0.868	0.817	0.799	0.811
$0.96 < m \leq 0.98$	0.817	0.786	0.778	0.815
$0.98 < m \leq 1.02$	0.706	0.706	0.747	0.796
$1.02 < m \leq 1.04$	0.678	0.651	0.715	0.784
$1.04 < m$	0.748	0.663	0.737	0.823
Panel H		HARGL/HARG Price RMSE		
$m < 0.94$	0.924	0.924	0.937	0.951
$0.94 < m \leq 0.96$	0.923	0.933	0.953	0.972
$0.96 < m \leq 0.98$	0.938	0.952	0.966	0.975
$0.98 < m \leq 1.02$	0.979	0.975	0.977	0.978
$1.02 < m \leq 1.04$	0.984	0.977	0.971	0.969
$1.04 < m$	0.949	0.940	0.943	0.949

Table 6: Option pricing performance on S&P500 out-of-the-money options from January 1, 1996 to December 31, 2004, computed with the CRV measure estimated from 1990 to 2007. We use the maximum likelihood parameter estimates from Table 1. Panel A: percentage price root mean squared error ($RMSE_p$) of the HARGL model sorted by moneyness and maturity. Panels B to F: $RMSE_p$ of the benchmark models relative to the HARGL sorted by moneyness and maturity. Maturity is in days and moneyness $m = K/S_t$, where K and S are the strike and underlying price, respectively.

	$1990-2007$		$1985-2007$	
	$RMSE_{IV}$	$RMSE_P$	$RMSE_{IV}$	$RMSE_P$
CRV	3.8546	0.0058	3.7208	0.0054
CRV/TS	0.9590	0.9061	0.7552	0.7013
CRV/RV5min	0.9431	0.8923	0.7519	0.7013

Table 7: HARGL model robustness of the option pricing results to different RV measures and different estimation periods. The table reports the absolute (first row) and relative (second and third rows) $RMSE_{IV}$ and $RMSE_p$, computed with three RV measures over two estimation periods. The three different RV measures are the five-minute return RV (RV5min), the Two-Scale estimator (TS), and the continuous component of the TS measure (CRV) obtained using the Threshold Bipower variation (see Section 3.2.). The two estimation periods are 1985-2007 and 1990-2007, while the pricing period remains from January 1, 1996 to December 31, 2004.

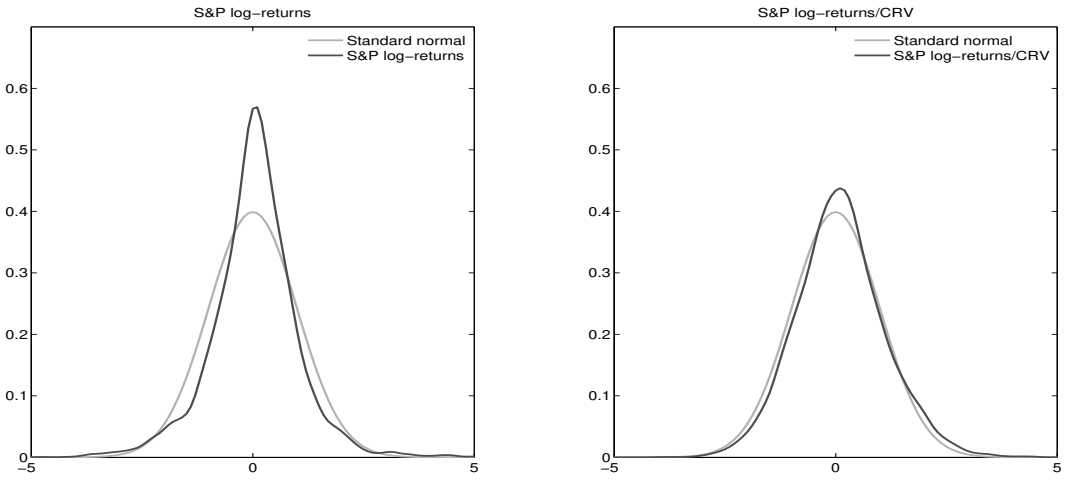

Figure 1: Log-returns distribution. Comparison of the S&P 500 index log-return distribution under different re-scaling measures. Left panel: Standard Normal distribution (grey line) and log-return rescaled by the sample standard deviation (black line). Right Panel: Standard Normal distribution (grey line) and log-return divided by contemporaneous realized volatility (black line).

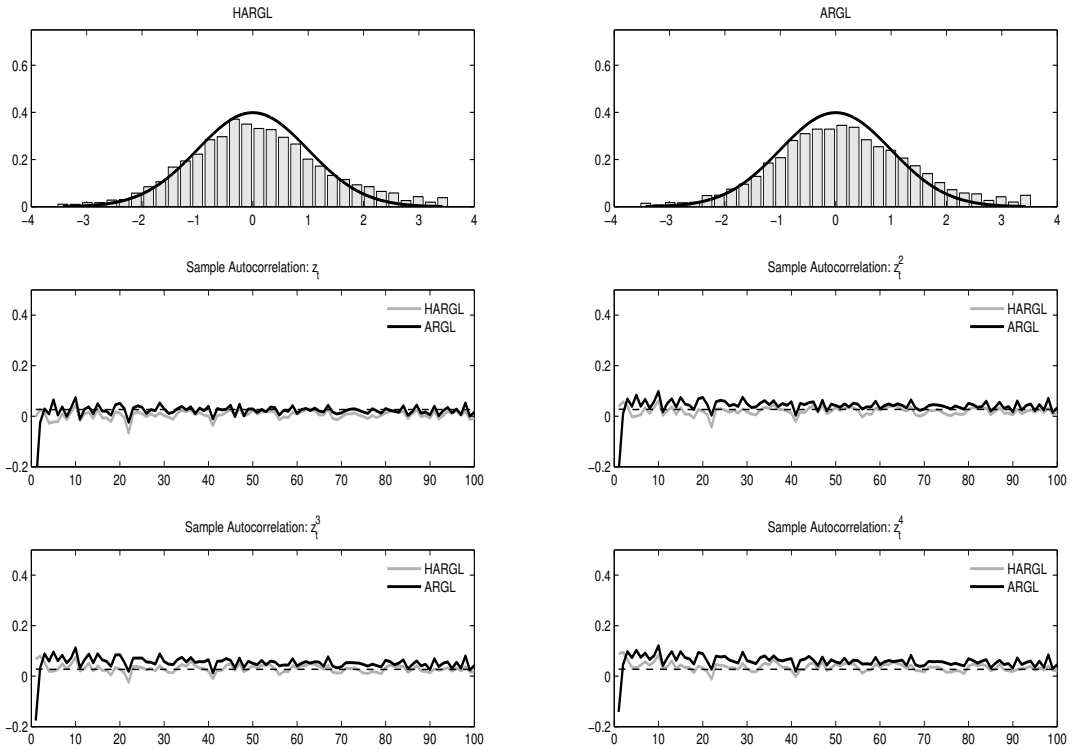

Figure 2: Model misspecification tests. The top panels show the histogram of $z_t = N^{-1}(P_{RV}(RV_t \leq \mathrm{rv}_t|\mathcal{F}_{t-1}, \hat{\theta}))$, where $\hat{\theta}$ represents the Maximum Likelihood Estimator for the considered stochastic volatility model. The smooth line represents the probability density function of a $N(0,1)$. The left panel is for the HARGL and the right panel is for the ARGL. The middle and bottom panels show the Sample Auto Correlation Function of $(z_t - \bar{z})$ (left middle panel), $(z_t - \bar{z})^2$ (right middle panel), $(z_t - \bar{z})^3$ (left bottom panel), and $(z_t - \bar{z})^4$ (right bottom panel). In each panel, the light line is for the HARGL, while the dark line is for the ARGL. The straight, dotted line in each plot is the Bartlett heteroskedasticity corrected upper bound at 95%-level of significance for the autocorrelation coefficients.

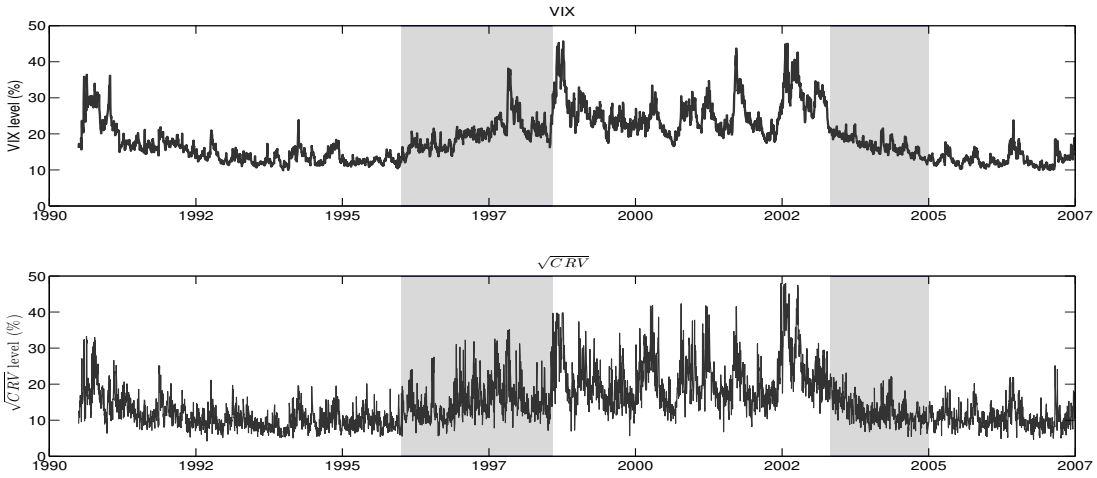

Figure 3: Volatility regimes. Plot of the CBOE volatility index (VIX) (top panel) and of the $\sqrt{CRV}$ measure (bottom panel) from January 1, 1990 to December 31, 2004. We identify three different volatility regimes: medium volatility from January 1, 1996 to August 1, 1998, high volatility from August 2, 1998 to May 1, 2003, and low volatility from May 2, 2003 to December 31, 2004.

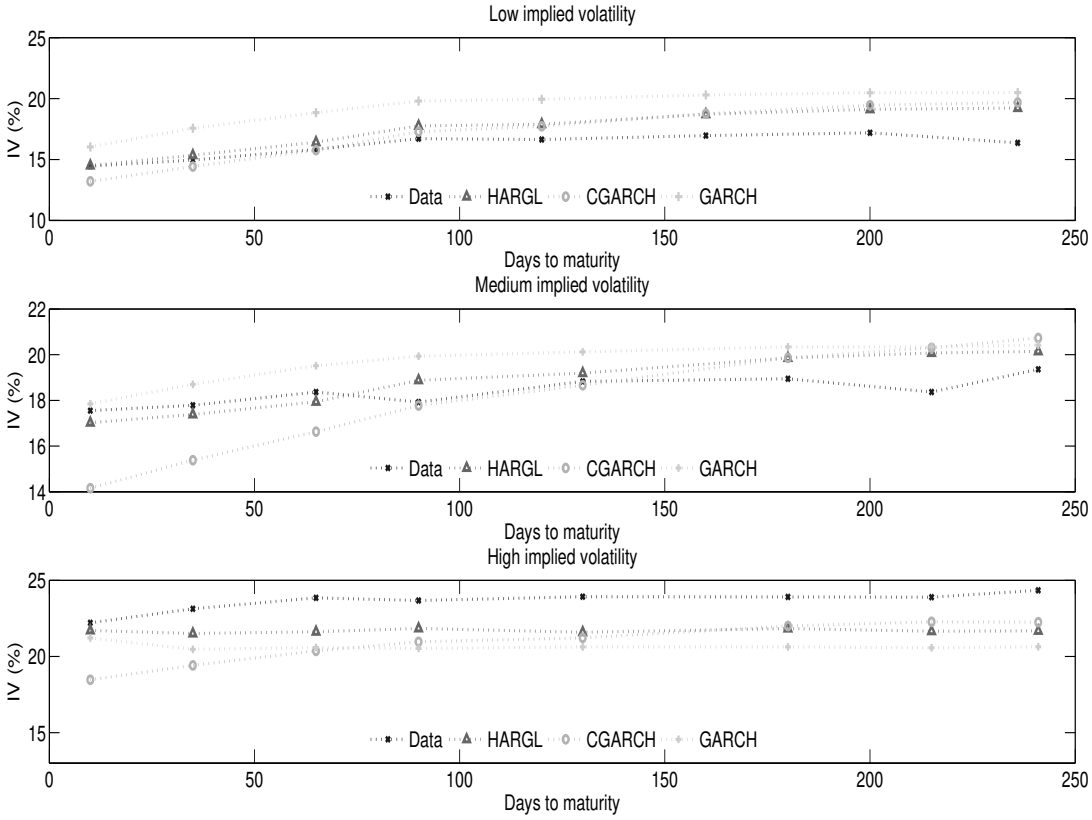

Figure 4: Implied volatility term structure for at-the-money options (with moneyness $m = K/S_t$ between 0.95 and 1.05, where K and S are the strike and underlying price, respectively). A dot represents the market-implied volatility, a triangle, the HARG model, a circle, the CGARCH model, and a cross, the GARCH model. The top, mid, and bottom panels correspond to the low, medium, and high-volatility regimes as detected in Figure 3. The parameter estimates are taken from Table 1.

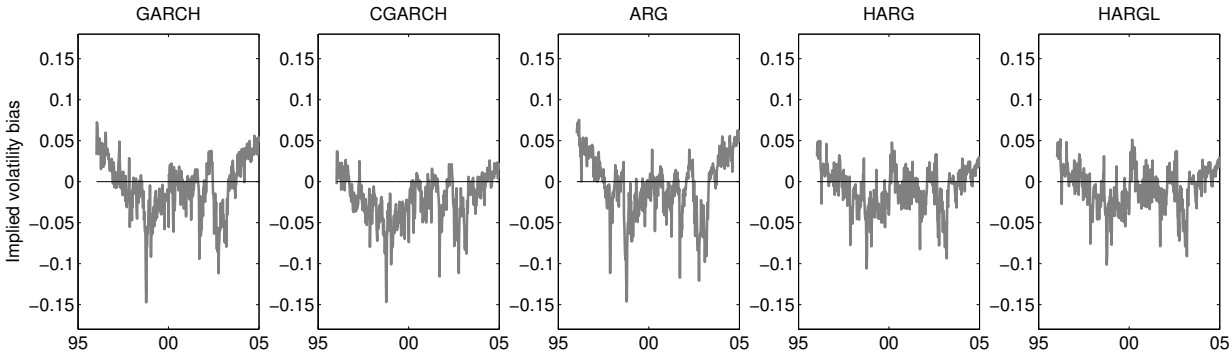

Figure 5: Weekly at-the-money options implied volatility bias. Plot of the average differences between the model and the market-implied volatility for at-the-money options (with moneyness $m = K/S_t$ between 0.95 and 1.05, where K and S are the strike and underlying price, respectively). The parameter estimates are taken from Table 1.

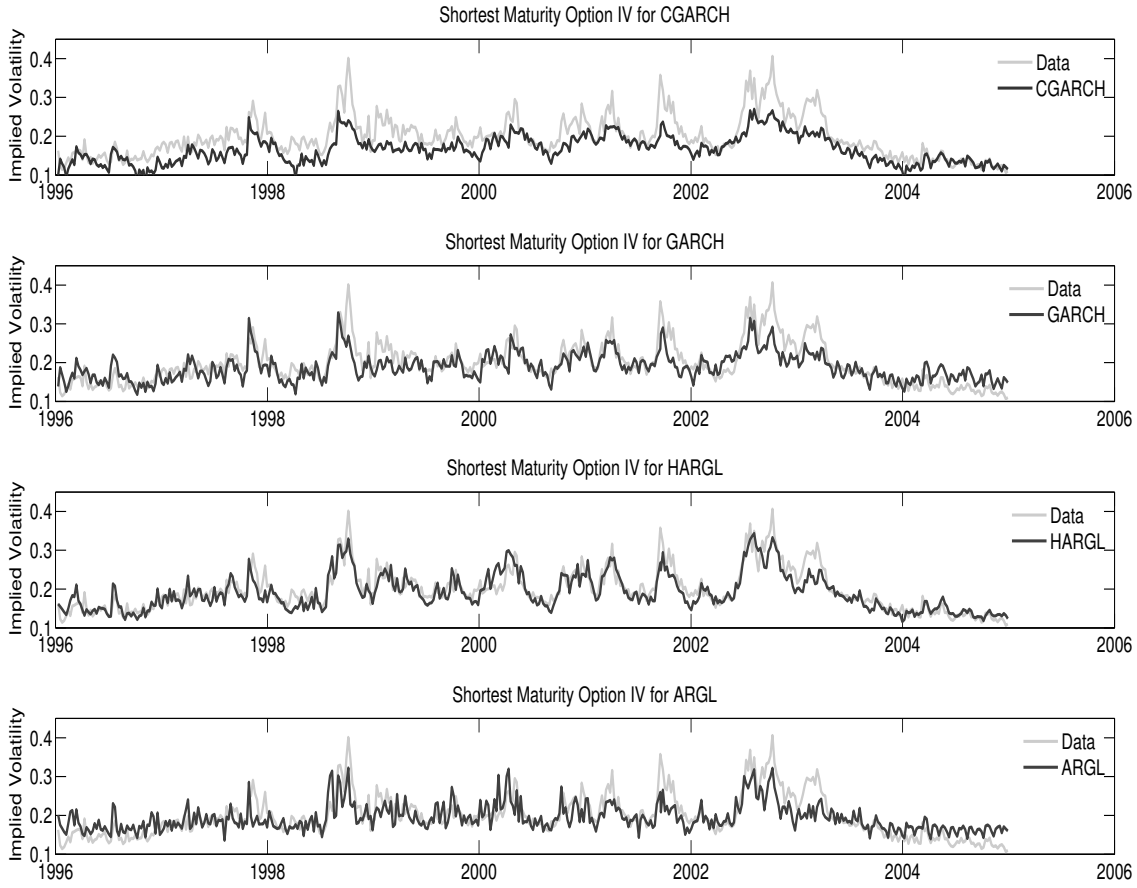

Figure 6: Level Dynamic from January 1, 1996 to December 31, 2004. Level is the average implied volatility of at-the-money options (with moneyness $m = K/S_t$ between 0.95 and 1.05, where K and S are the strike and underlying price, respectively) and maturity the shortest available on a given day. In each panel, the light line represents the data, the black line, the model. The top panel illustrates the performance of the CGARCH, the second panel refers to the GARCH model, while the third and the bottom panels refer to the HARGL and ARGL, respectively. The parameter estimates are taken from Table 1.

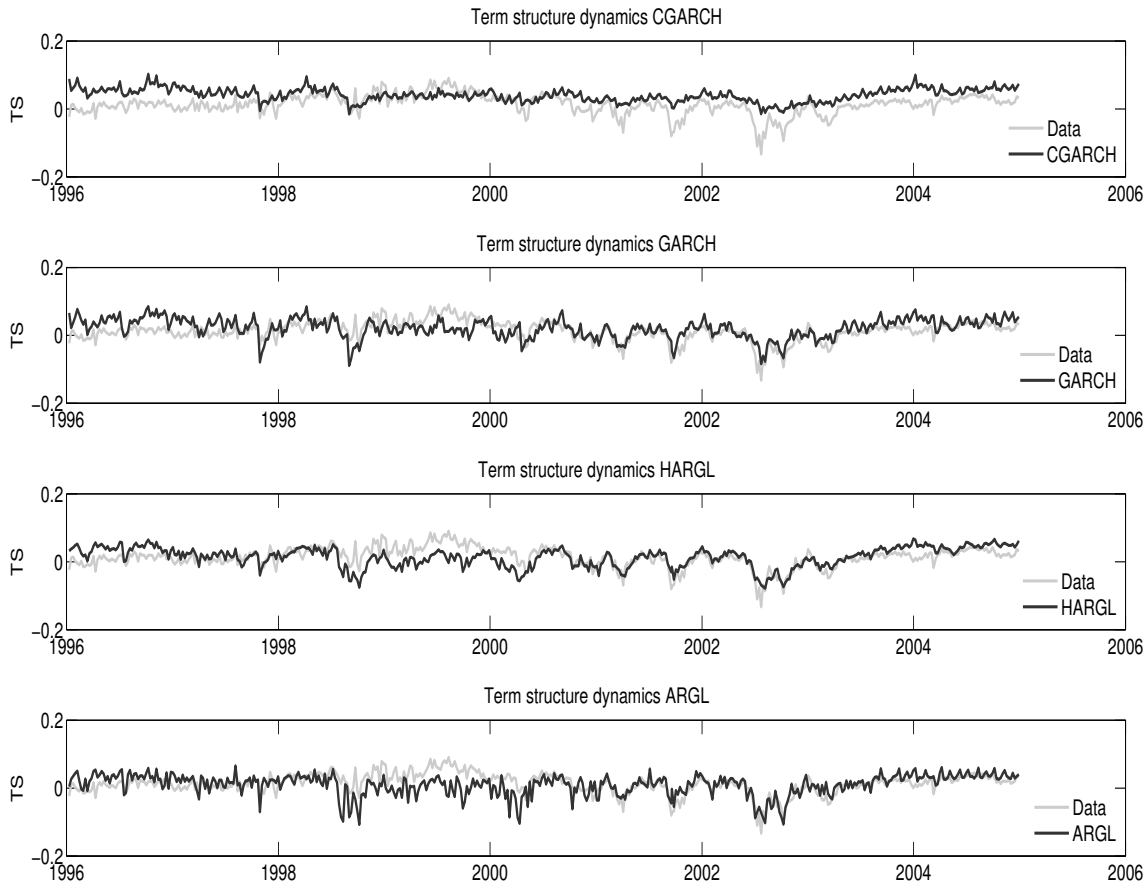

Figure 7: Term Structure Dynamic from January 1, 1996 to December 31, 2004. Term structure represents the slope of the implied volatility surface and is given by the difference between the average implied volatility of at-the-money (with moneyness $m = K/S_t$ between 0.95 and 1.05, where K and S are the strike and underlying price, respectively) long maturity (more than 120 days) options and level. In each panel, the light line represents the data, and the black line represents the model. The top panel illustrates the performance of the CGARCH, the second panel refers to the GARCH model, while the third and the bottom panels refer to the HARGL and ARGL, respectively. The parameter estimates are taken from Table 1.

swiss:finance:institute

c/o University of Geneva
40 bd du Pont d'Arve
1211 Geneva 4
Switzerland

T +41 22 379 84 71
F +41 22 379 82 77
RPS@sfi.ch
www.SwissFinanceInstitute.ch